



U.S. DEPARTMENT OF
ENERGY

Nuclear Energy

Structure-Property Relationship in Metal-Organic Frameworks for Enhanced Energy Related Applications

Dorina F. Sava

Nanoscale Science Department
Sandia National Laboratories
Albuquerque, NM

Advanced Photon Source- Argonne National Laboratory
June 26, 2012



Sandia National Laboratories

Acknowledgements

Sandia National Laboratories

Tina M. Nenoff

Mark A. Rodriguez

Lauren E. S. Rohwer

Terry J. Garino

David X. Rademacher

Jeffery A. Greathouse

Paul Crozier

Argonne National Laboratory

Karena W. Chapman

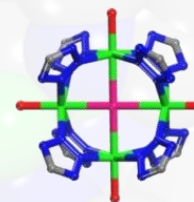
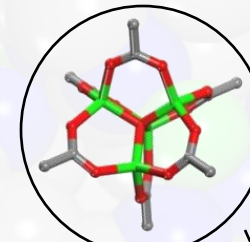
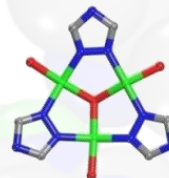
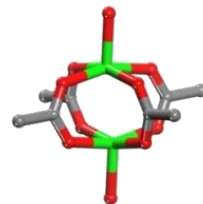
Peter J. Chupas

Gregory Halder

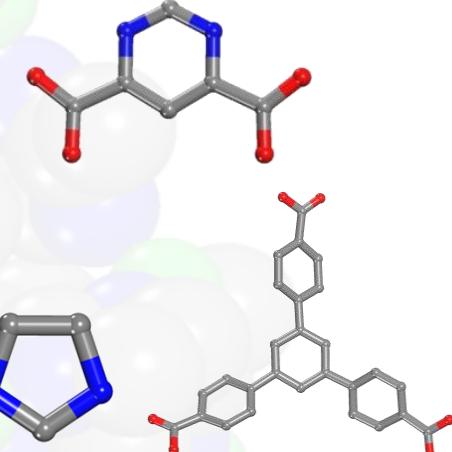
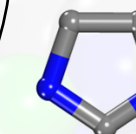
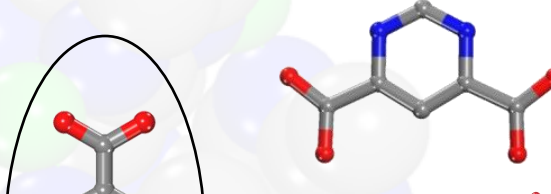
This project is funded under the DOE/NE-FCR&D Separations and Waste Form Campaign;
SAND Number: 2012-5262 C

Sandia National Laboratories is a multiprogram laboratory managed and operated by Sandia Corporation, a wholly owned subsidiary of Lockheed Martin Corporation, for the U.S. Department of Energy's National Nuclear Security Administration under contract DE-AC04-94AL85000.

MOFs are highly crystalline materials constructed from metal nodes and organic linkers



Common metal clusters
(molecular building blocks)



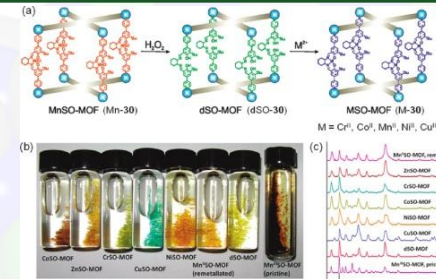
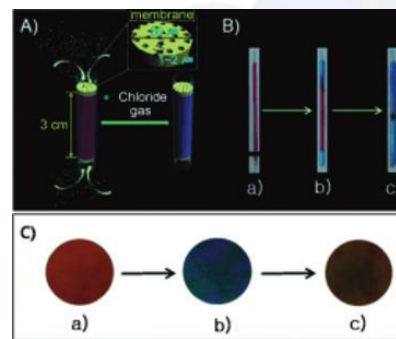
Organic linking units



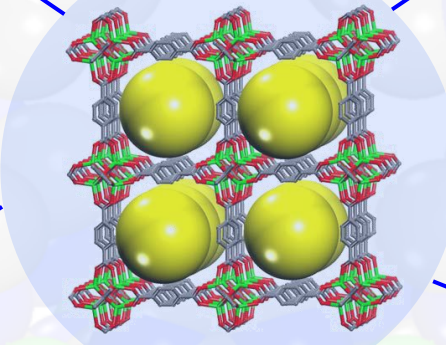
MOFs are versatile materials that span diverse applications

Chem. Rev. 2012, 112, 673-1268.

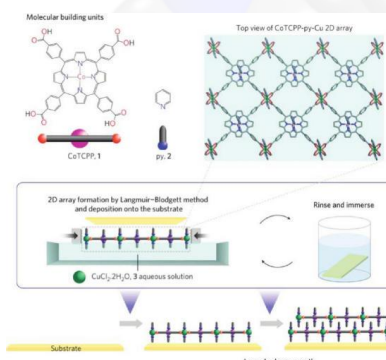
Sensors



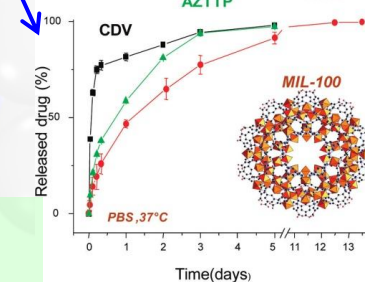
Catalysis



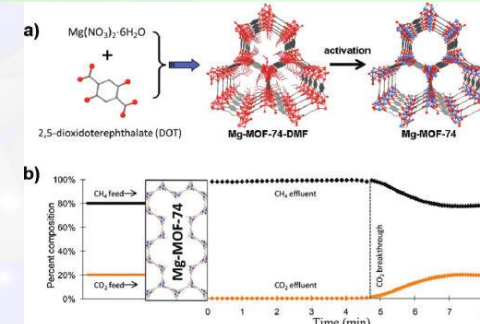
Membranes



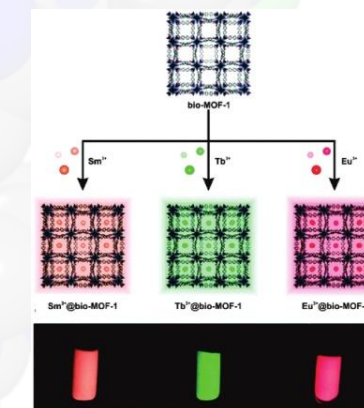
Biomedicine-drug delivery



Gas storage and separations

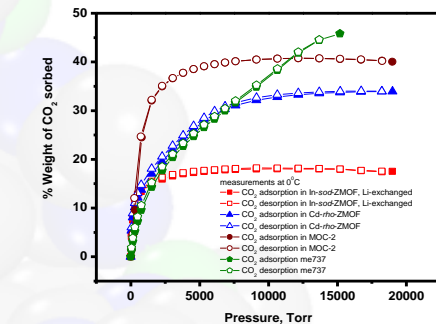
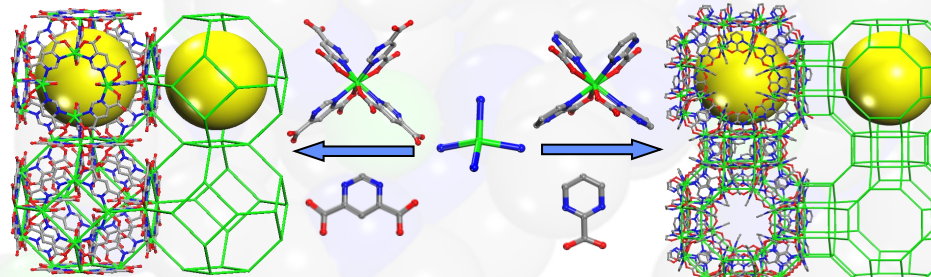


Luminescence

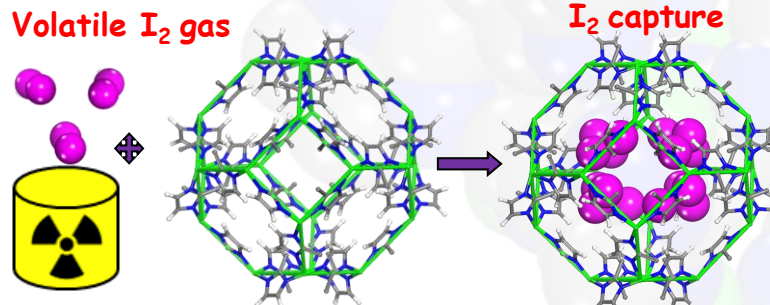


Outline

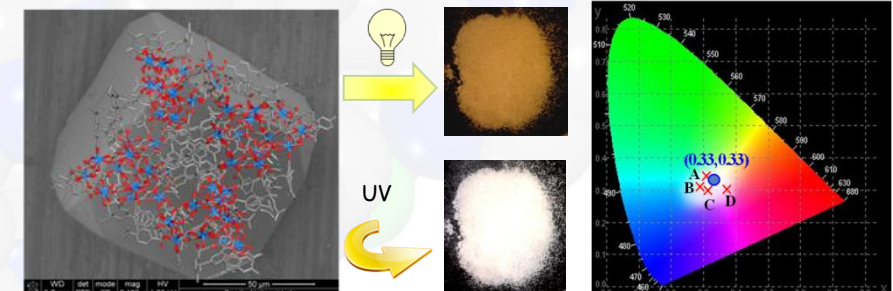
I. Design strategies for the rational construction of MOFs with zeolitic topologies



II. Capture and Storage of Volatile Fission Gas Products from Reprocessing and/or Nuclear Accidents



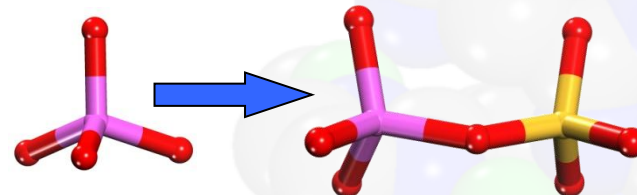
III. Novel MOFs with Tunable Color Properties



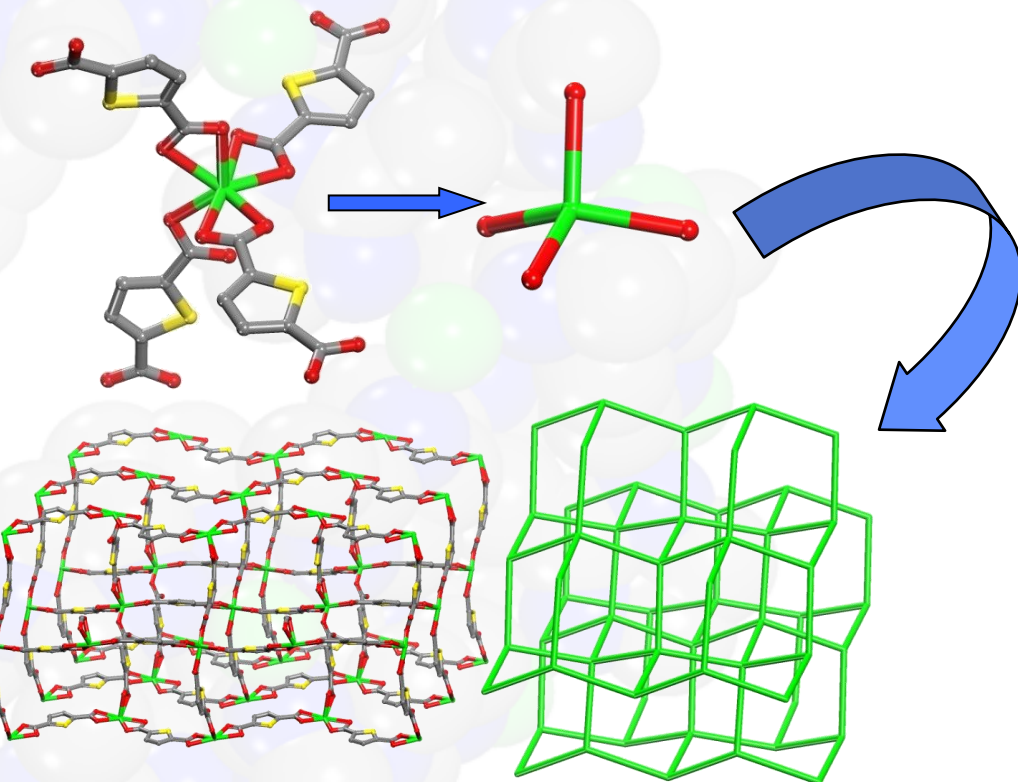
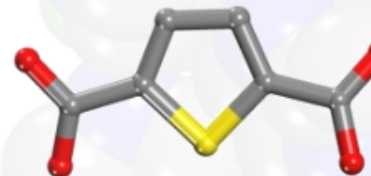
I. Design strategies for the construction of MOFs with zeolitic topologies

Top-down design and bottom-up approach for the "edge expansion" strategy for the construction of the metal-organic zeolitic analogues

Tetrahedral node=TO₄



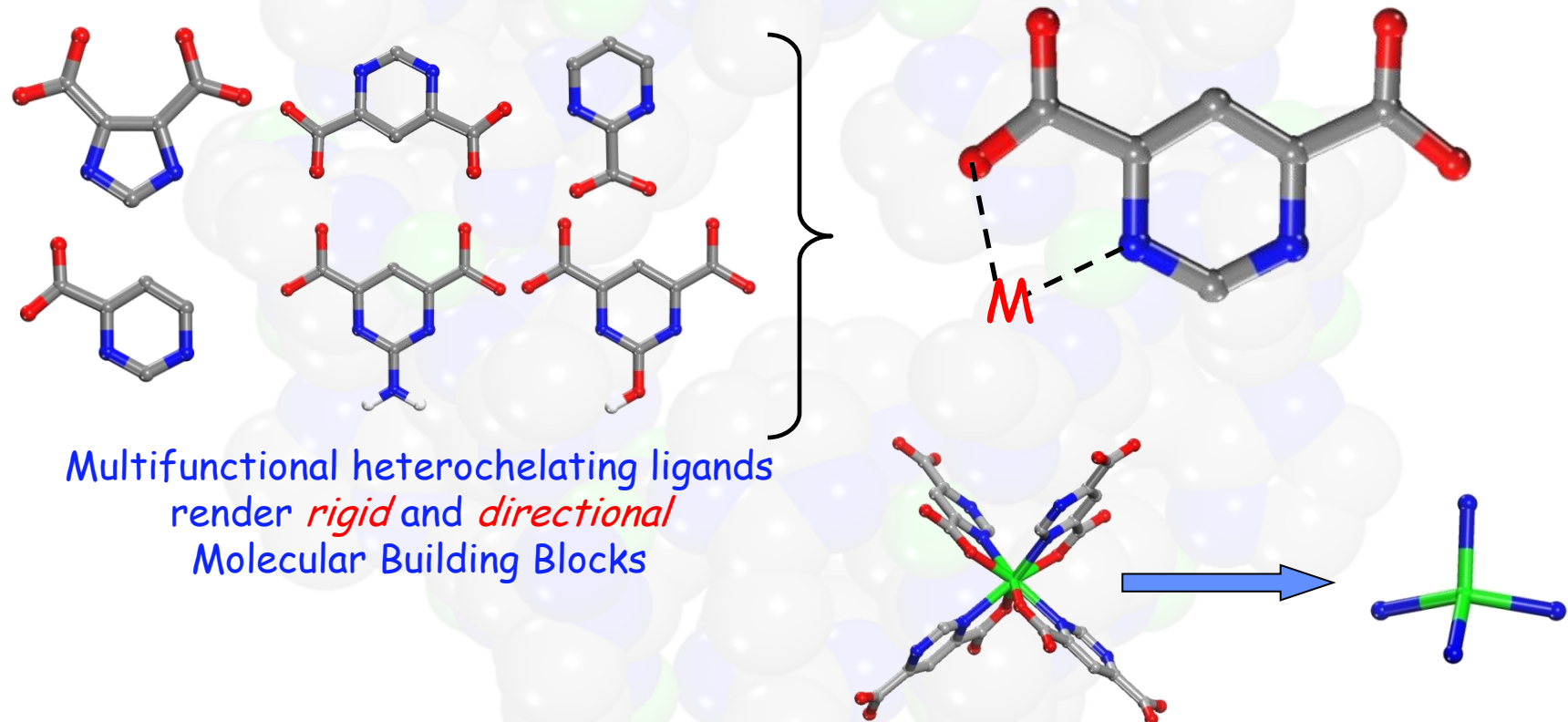
T-O-T=145°



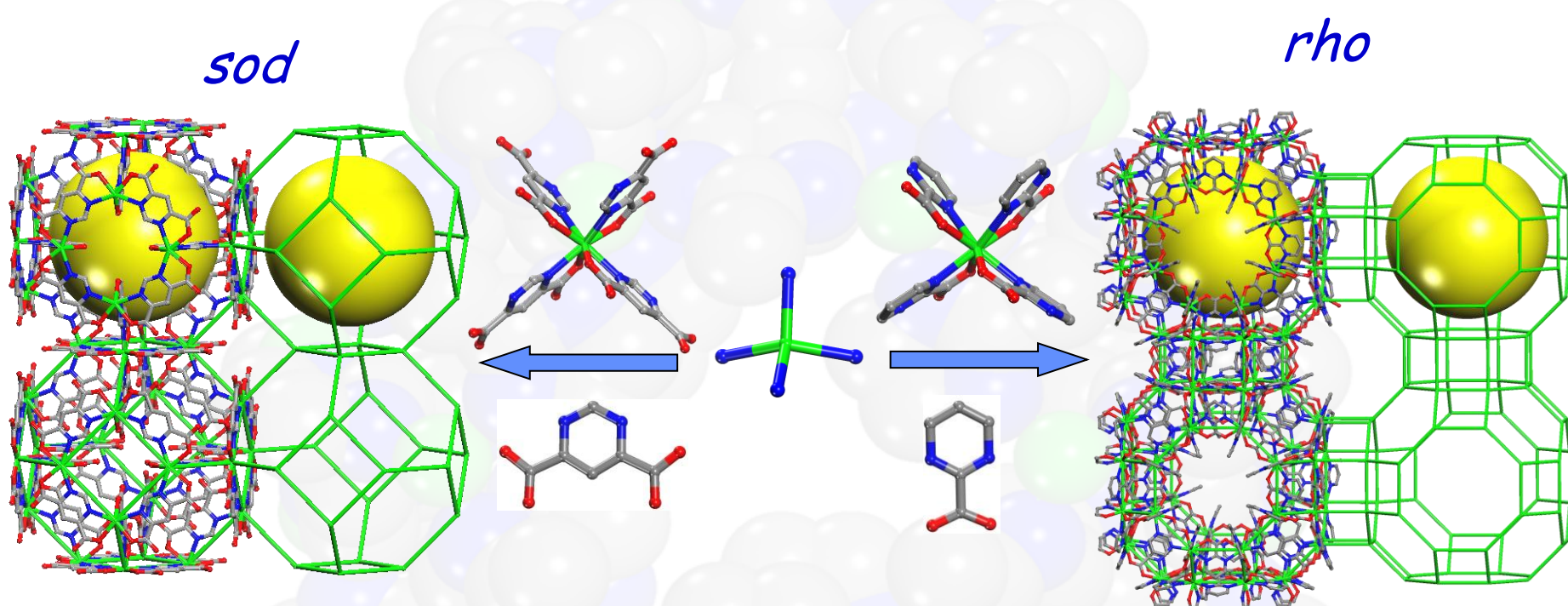
MBB flexibility prevents targeted net formation - default net is preferred

Alternative approach via *rigid* and *directional* Tetrahedral Building Blocks

The deliberate construction of porous periodic solids, utilizing the single-metal-ion-based approach



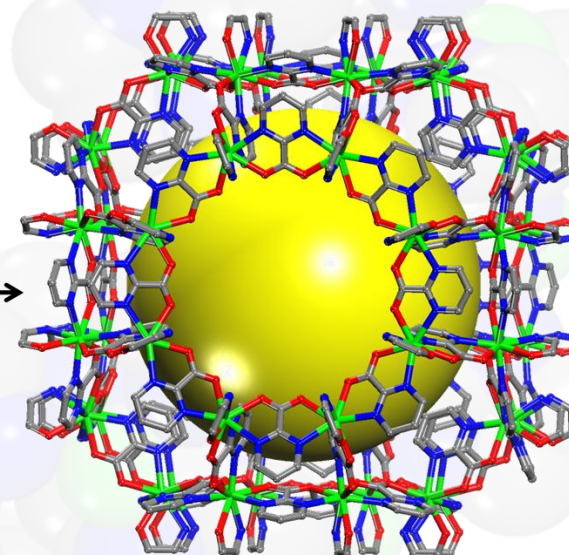
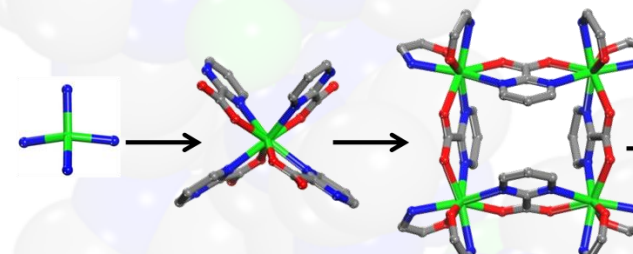
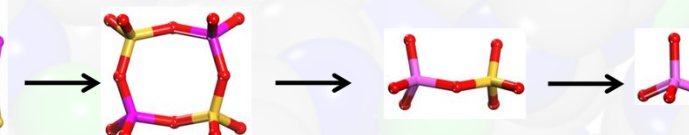
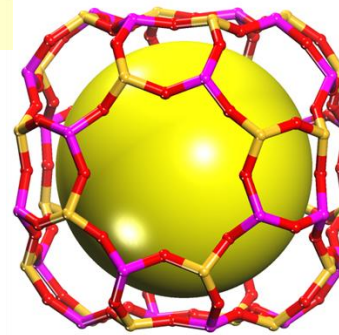
Ia. Zeolite-like Metal–Organic Frameworks from pyrimidinecarboxylate bis-chelating bridging ligands



- (i) forbidden self interpenetration- design of readily accessible extra large cavities
- (ii) chemical stability in water (not common in MOFs) - applications for heterogeneous catalysis, separations, and sensors
- (iii) tune extra framework cations toward specific applications & removal/sequestration of toxic metal ions

MOF zeolite *rho*: 8 times the volume and an order of magnitude higher surface area vs. inorganic RHO

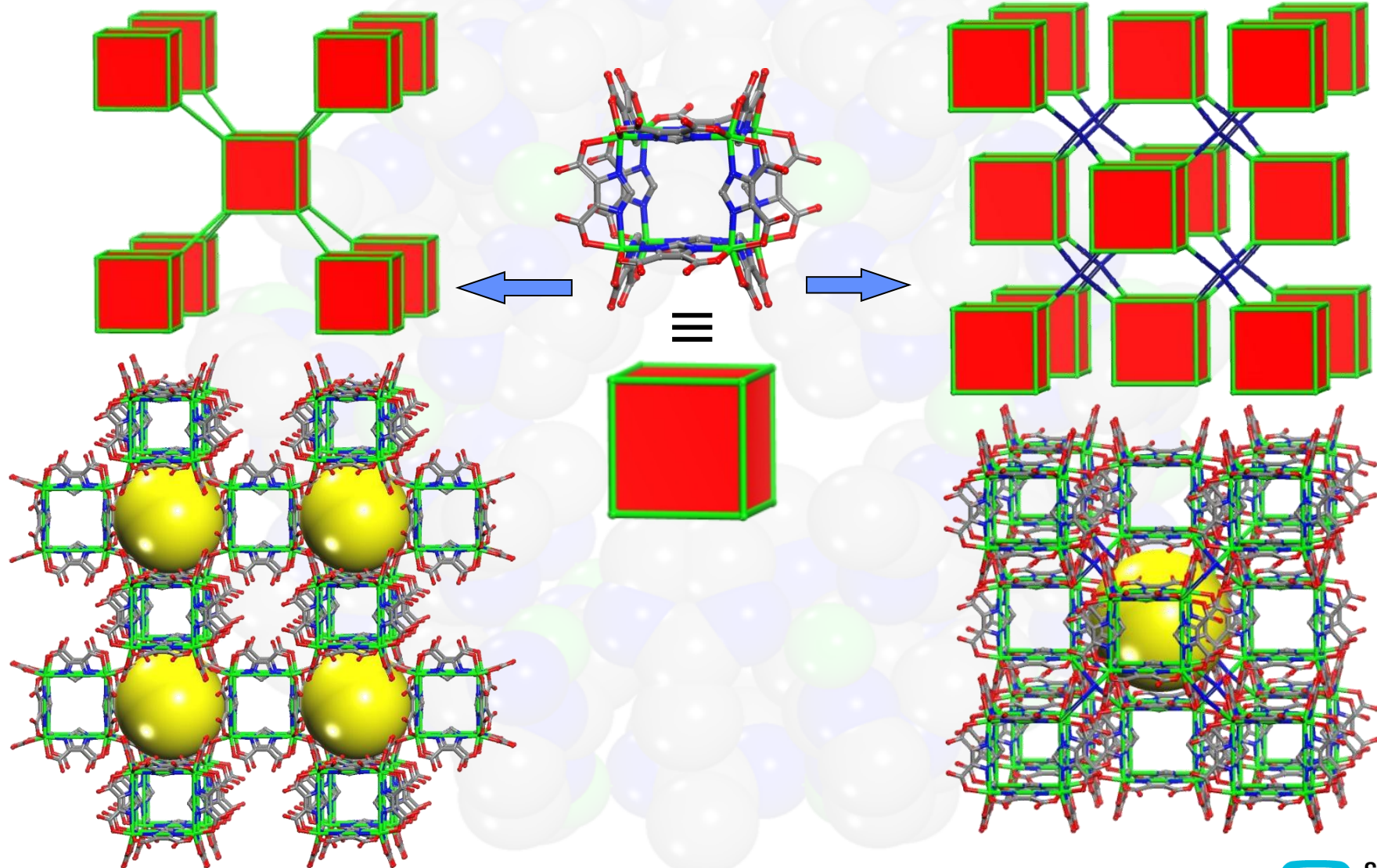
Zeolite RHO

Metal-organic
analogue *rho*

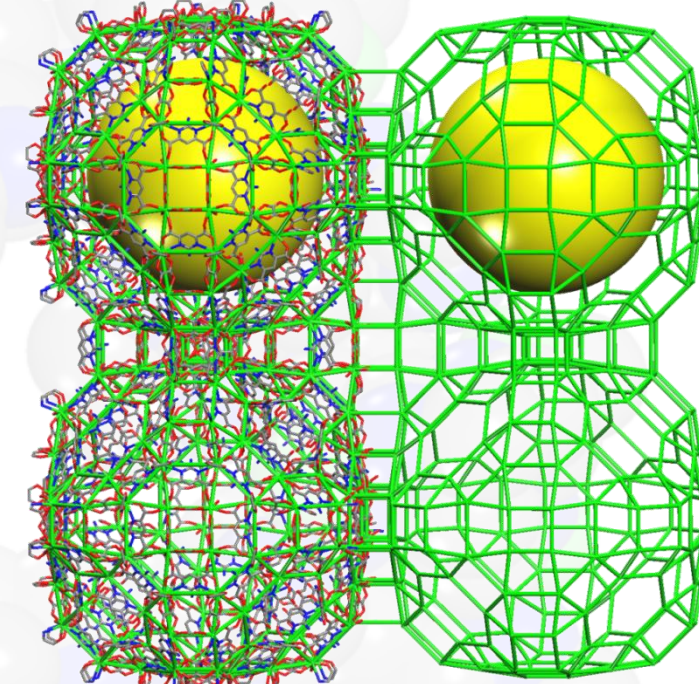
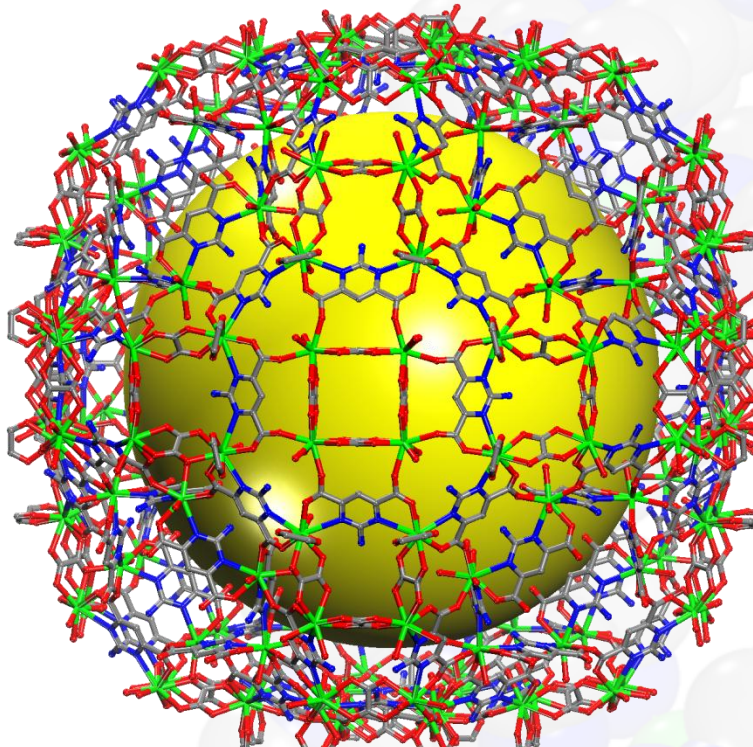
- The unit cell volume of the MOF *rho* framework is ~ **8 times larger** than the alumino-silicate analogue- unit cell edge is doubled (3 nm vs. 1.5 nm)

- Apparent surface area:
inorganic RHO ~ 100-200 m²/g
MOF *rho* ~ 1100- 1800 m²/g

Ib. MOFs with zeolitic topologies constructed from the assembly of Metal-Organic Cubes



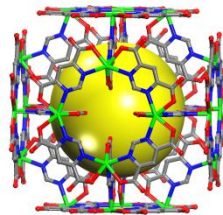
Ic. Zeolite-like MOFs with extra-large cavities



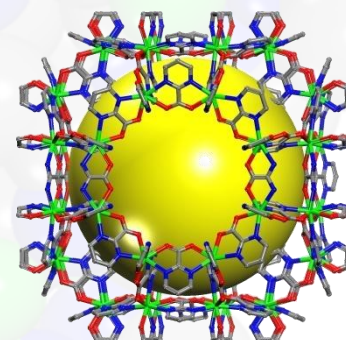
diameter of ~38 Å

| Material | Inner diameter | Outer diameter | Metal atoms per cage |
|-----------|----------------|----------------|----------------------|
| This work | 38 Å | 48 Å X 53 Å | 168 |
| Mes.MOF-1 | 47.1 Å | 59.5 Å | 84 |
| MIL-101 | 33.8 Å | 46.7 Å | 126 |
| ZIF-100 | 35.6 Å | 67.2 Å | 264 |

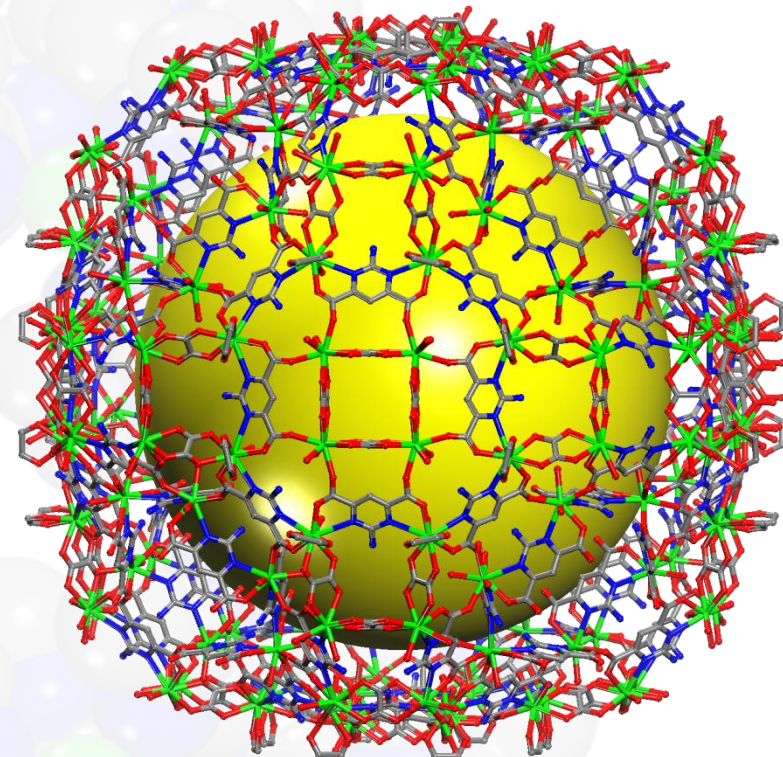
Systematic variation of the organic components leads to increased complexity



sod- diameter
of $\sim 9.6\text{\AA}$

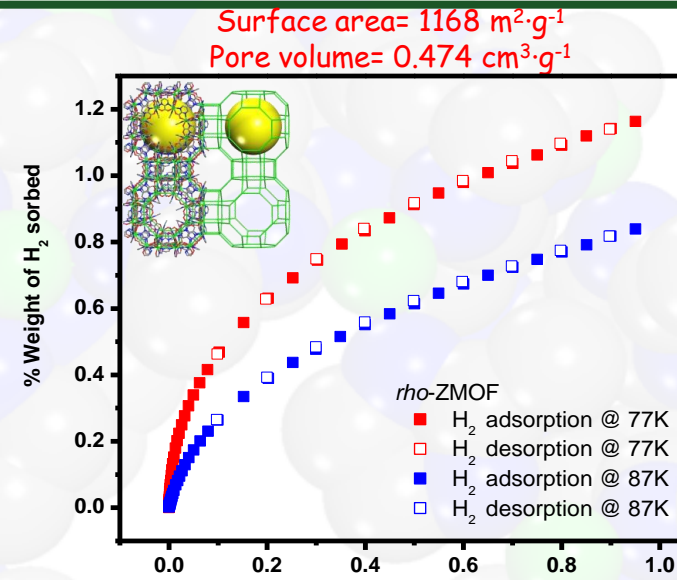
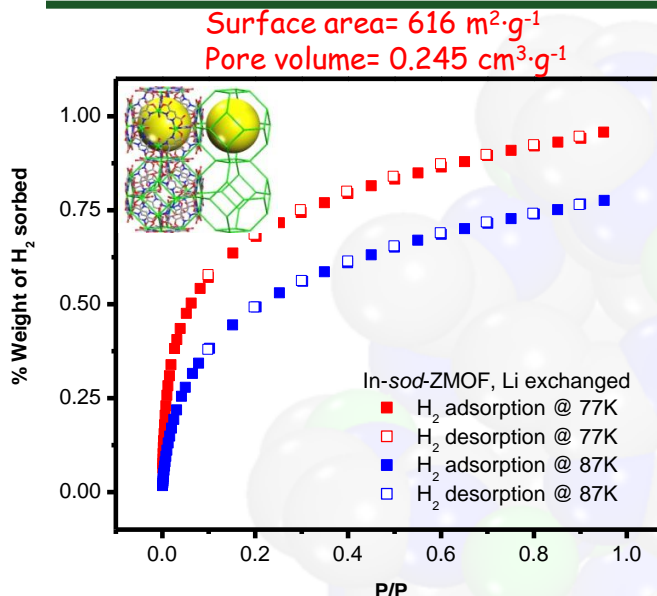


rho - diameter
of $\sim 16.4\text{\AA}$

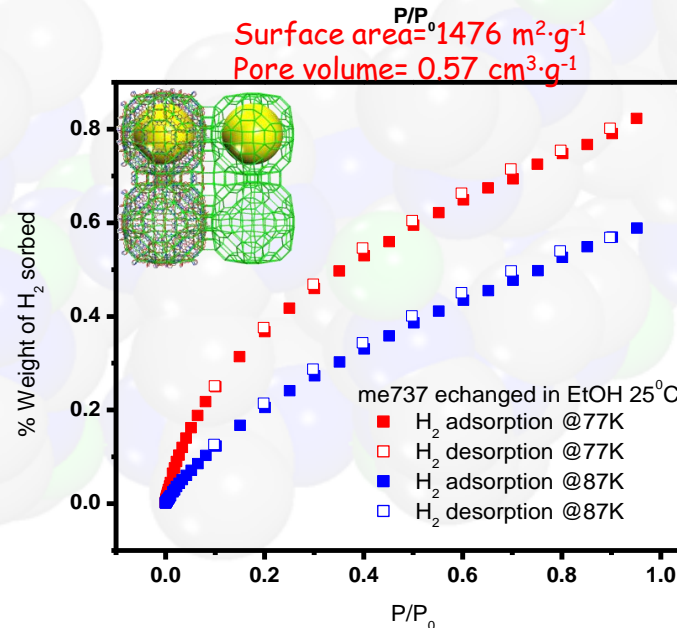
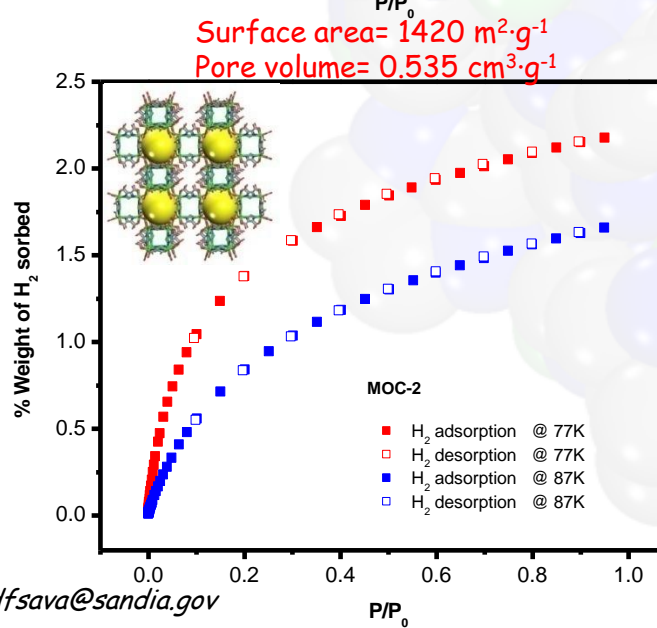


diameter
of $\sim 38\text{\AA}$

H_2 sorption isotherms

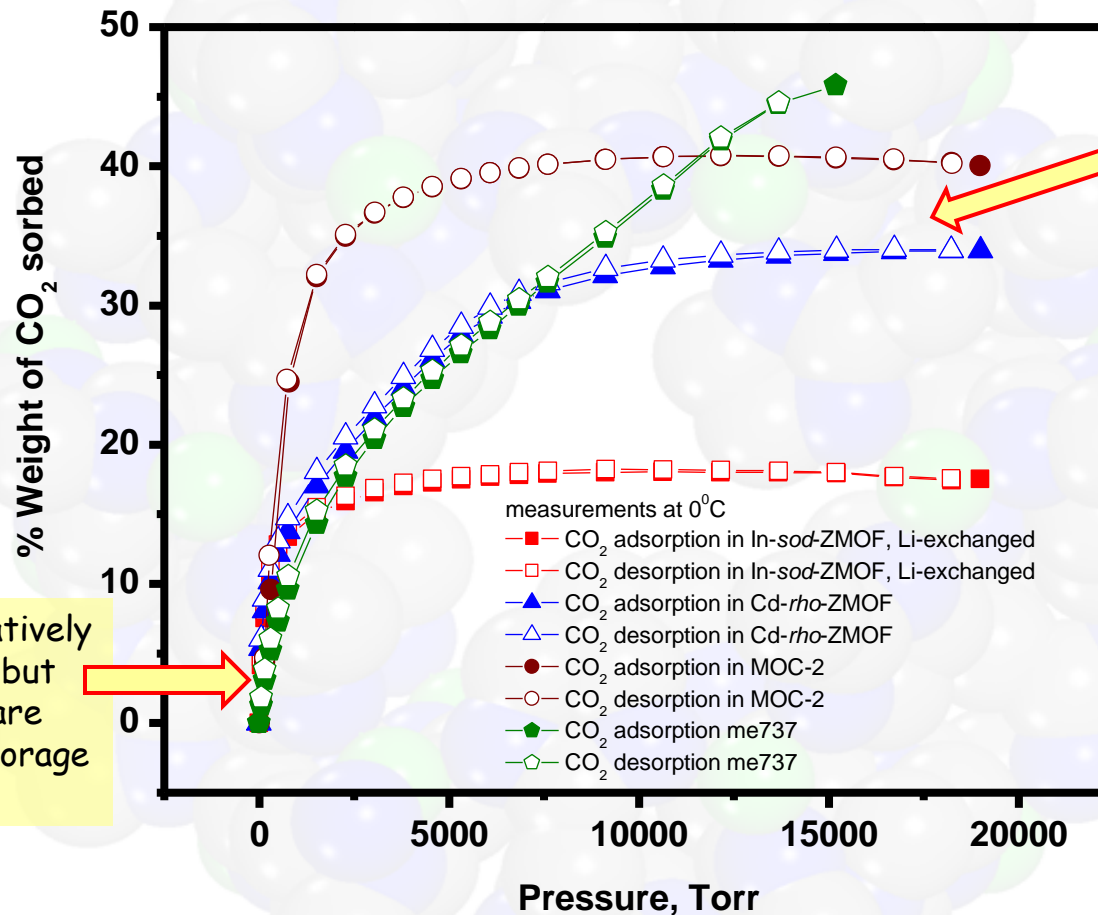


H_2 storage is dependant on surface area, pore size and pore volume, as well as on additional favorable sites for the gas adsorption to increase binding affinities



Materials with high local charge densities increase the binding affinities between H_2 and framework

CO₂ sorption isotherms measured at 273K

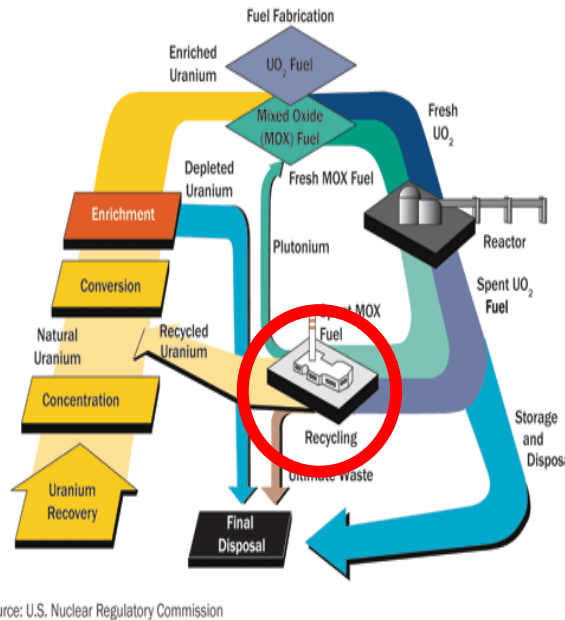


Compounds with both large and extra-large cavities and high pore volumes- important for applications conducted at high pressures

Materials with relatively narrow pore sizes, but large pore volume are suitable for CO₂ storage at low pressure

II. Capture and Storage of Volatile Fission Gas Products from Reprocessing and/or Nuclear Accidents

Nuclear Fuel Reprocessing (NE)



Accidental Release



Fukushima Daiichi Nuclear Power Plant explosion; March 11, 2011
 I^{129} , I^{131} volatile gas released
(www.IAEA.org)

The importance of capturing volatile radioactive iodine (I_2) gas

- **Appropriate nuclear waste management:** a main concern for safety associated with nuclear energy
- Particularly challenging is the capture of volatile gaseous fission products from nuclear fuel reprocessing or inadvertent environmental release: ^{129}I and ^{131}I , ^3H , $^{14}\text{CO}_2$, and ^{85}Kr
- Unique exposure problems for radio- I_2 isotopes:
 - ^{129}I : long-lived isotope (half-life of 1.57×10^7 years), requiring *capture and reliable storage while it decays*
 - ^{131}I : short-lived (half-life of 8.02 days), but *requires immediate capture* as it directly affects human metabolic processes

Judicious selection of an “ideal” candidate for I₂ sorption

Pre-requisites

- Restrictive pore apertures to impart molecular selectivity for directional diffusion of iodine ($\sim 3.35 \text{ \AA}$)
- Large surface area and pore volume
- High *chemical, thermal, and moisture stability*

Judicious selection of an “ideal” candidate for I₂ sorption

Pre-requisites

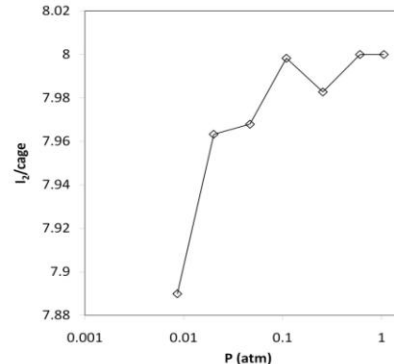
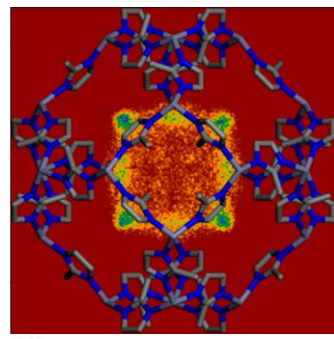
- Restrictive pore apertures to impart molecular selectivity for a directional diffusion of iodine ($\sim 3.35 \text{ \AA}$)
- Large surface area and pore volume
- High *chemical, thermal, and moisture stability*

ZIF-8: Zn(2-methylimidazole)₂

- ✓ β -cages= 11.6 \AA diameter,
Pore apertures $\sim 3.4 \text{ \AA}$
- ✓ Surface area ZIF-8 = 1,947 $\text{m}^2 \text{ g}^{-1}$
Pore volume= 0.663 cc g^{-1}
- ✓ Chemically stable in boiling solvents (including water), and thermally stable up to 550°C

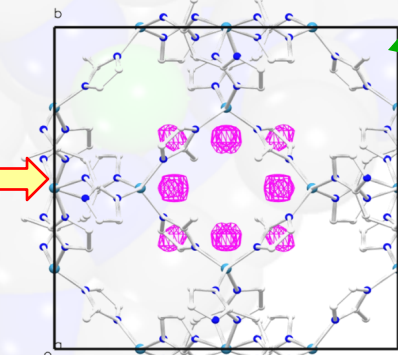
IIa. Establishing structure-function relationship: integration of experiment and modeling

Molecular modeling

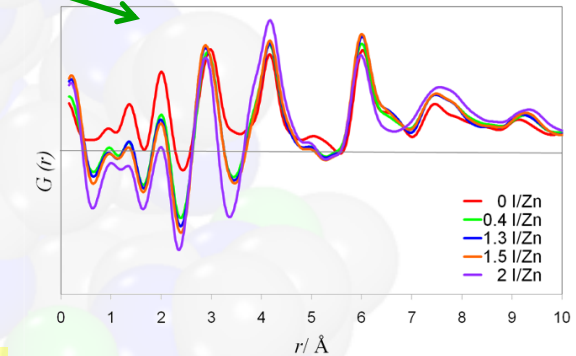


MD and GCMC simulations predict I_2 binding locations and maximum loading capacities

Complementary local and long-range structural probes



High-resolution synchrotron data:
Difference-Fourier analysis map
confirms I_2 location within cages

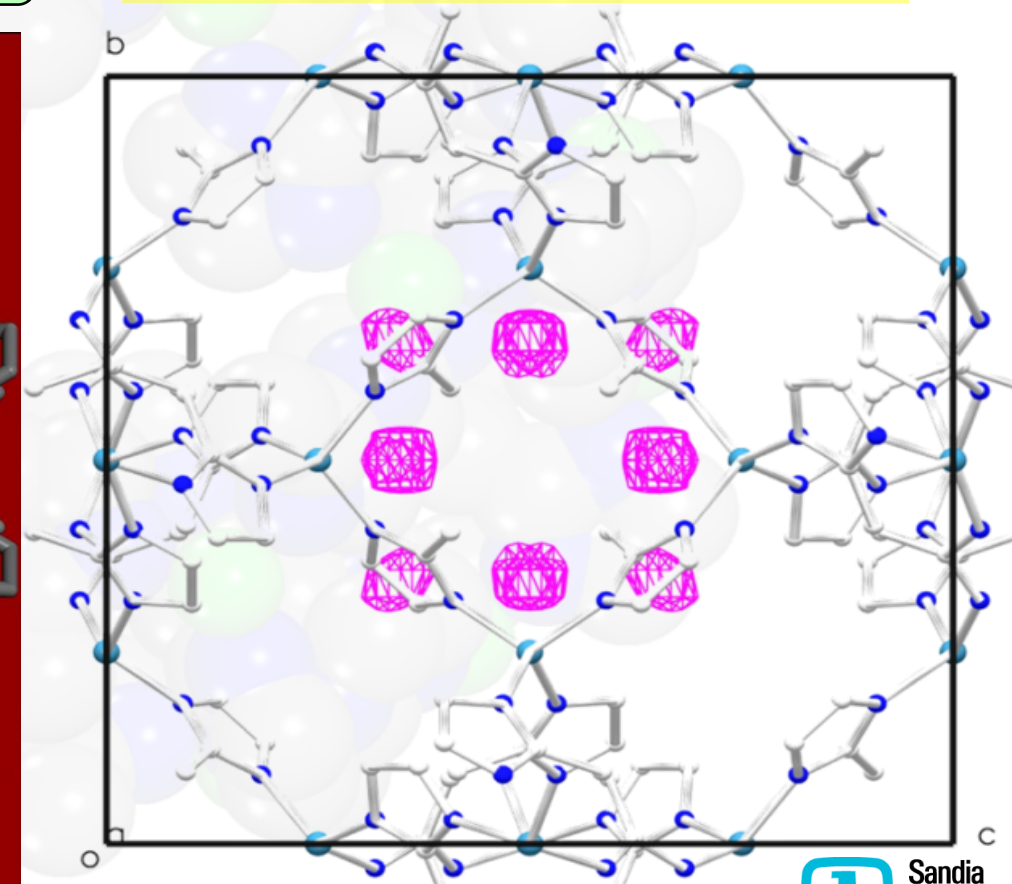
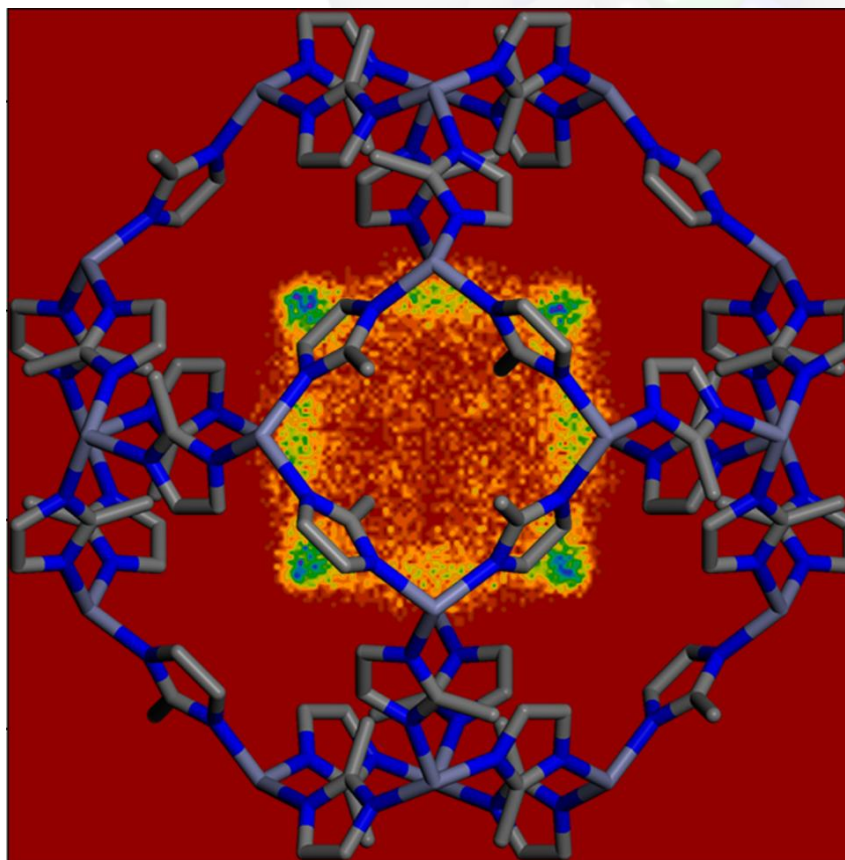


Pair Distribution Function
analysis: histogram of all
interatomic distances,
independent of sample
crystallinity

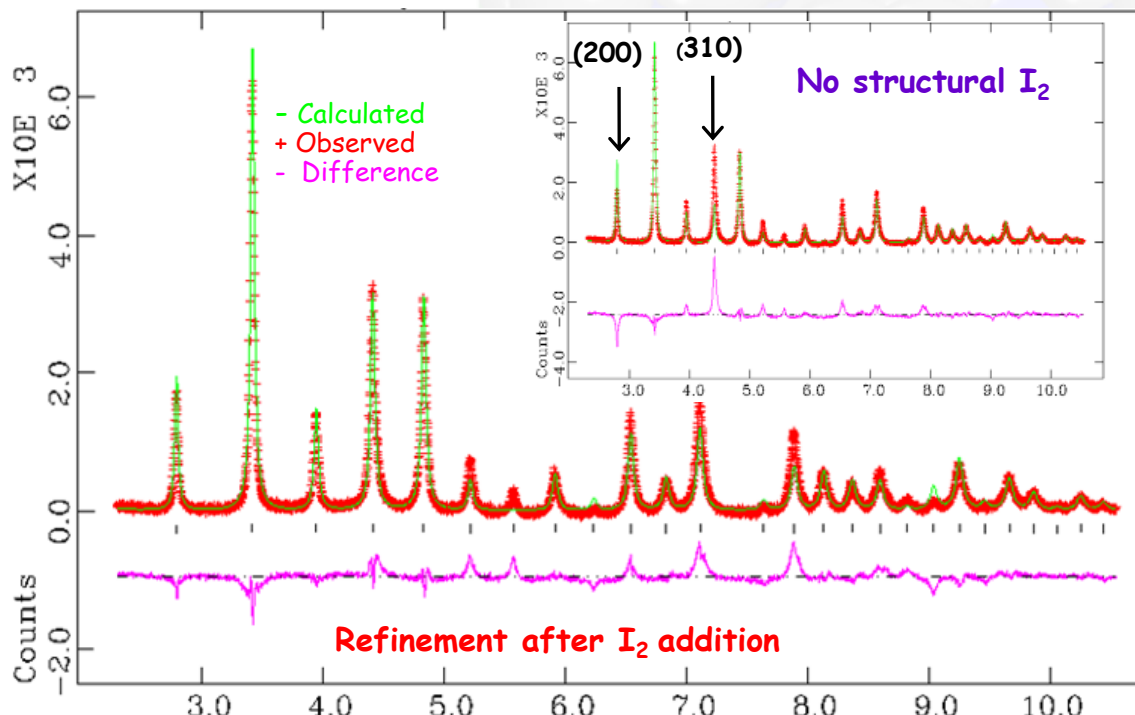
MD simulations predict I_2 location and loading capacities within ZIF-8 cage

2 I/Zn (~6 I_2 per cage)

Time-averaged atomic density plot:
increased density at positions closely
related to those indicated in the
Bragg analysis



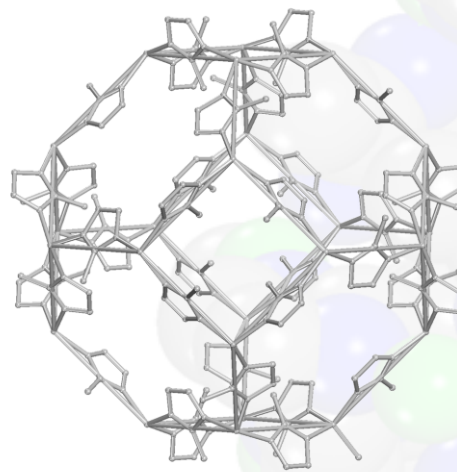
High-resolution synchrotron-based XRD



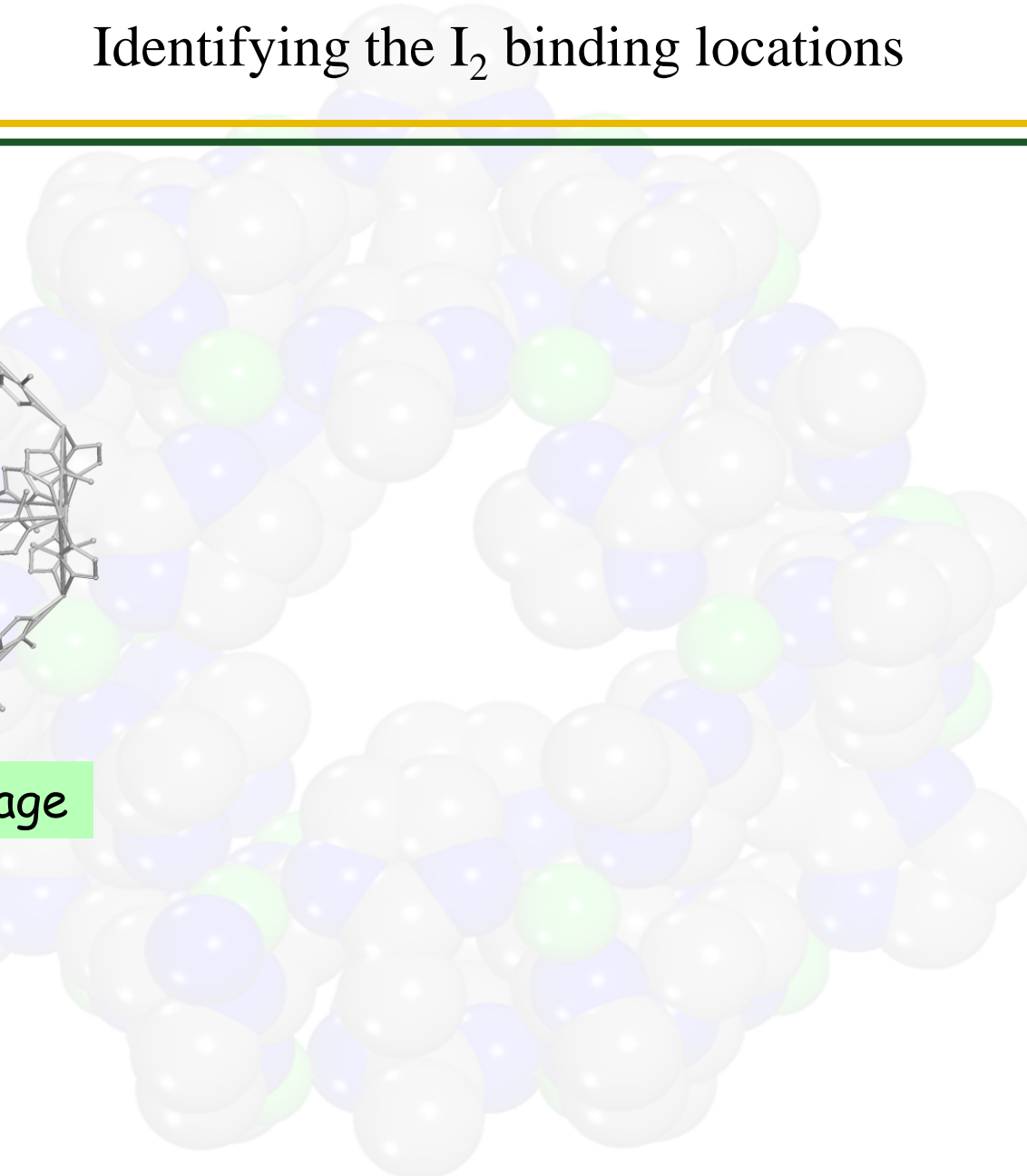
Calculated, observed and difference spectrum of 0.4
 I/Zn (25 wt.% I_2) loading of I_2 @ZIF-8 after I_2
inclusion in structure refinement by Rietveld analysis
(inset: before I_2 inclusion).

- Sample crystallinity is maintained up to $\sim 1.3 \text{ I}/\text{Zn}$ (70 wt.% I_2) loadings
- Bragg reflections broaden significantly beyond this value → difficult to distinguish from the pronounced diffuse features in the "background"
- Experimental maximum capacity is reached at $\sim 2 \text{ I}/\text{Zn}$ (110 wt.% I_2) loadings

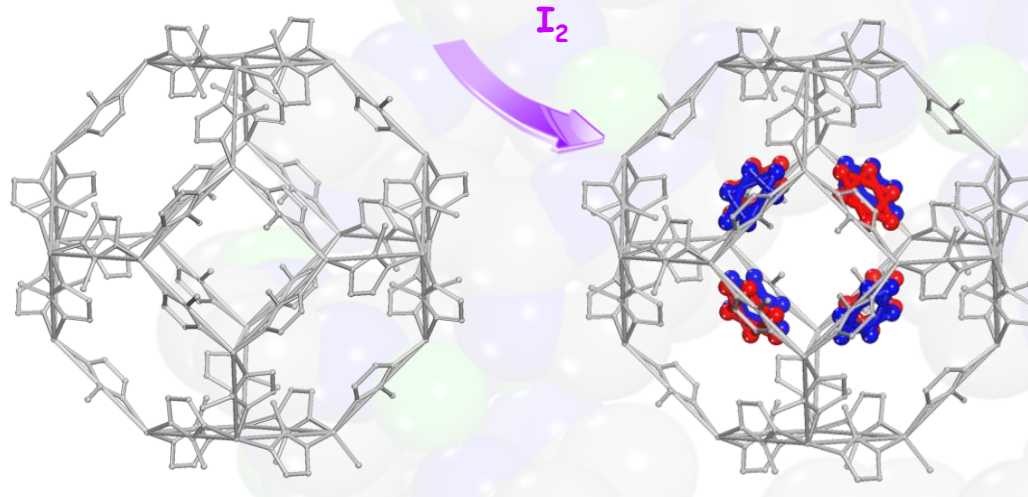
Identifying the I_2 binding locations



Activated β -cage



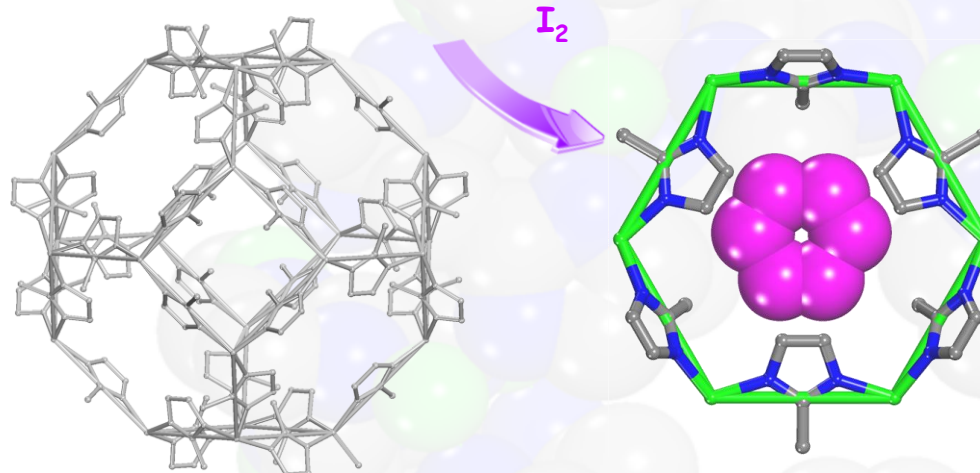
Identifying the I_2 binding locations



Activated β -cage

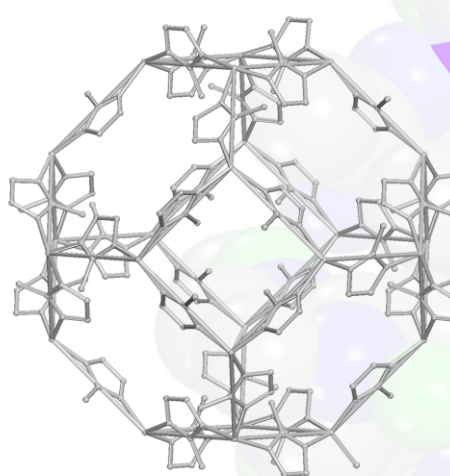
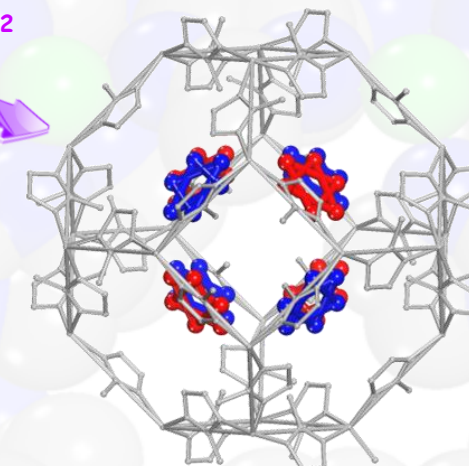
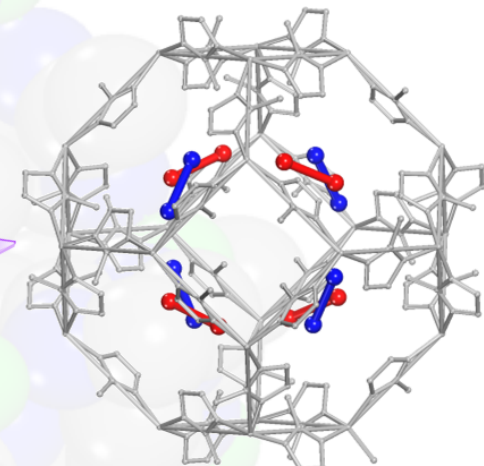
Dynamically disordered
 I_2 molecules

Identifying the I_2 binding locations



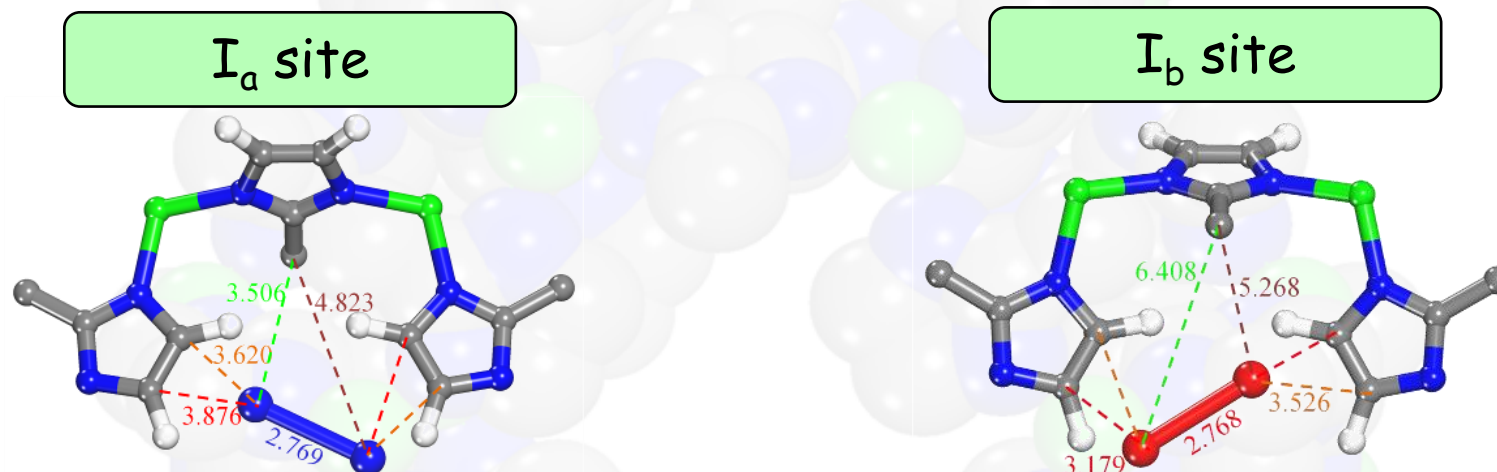
Activated β -cage

Dynamically disordered
 I_2 molecules

Identifying the I_2 binding locationsActivated β -cageDynamically disordered
 I_2 moleculesRefined I_2 sites:
 I_a (blue) and I_b
(red)

I_2 adsorption in ZIF-8 is due to favorable interactions with the 2-MeIM linker

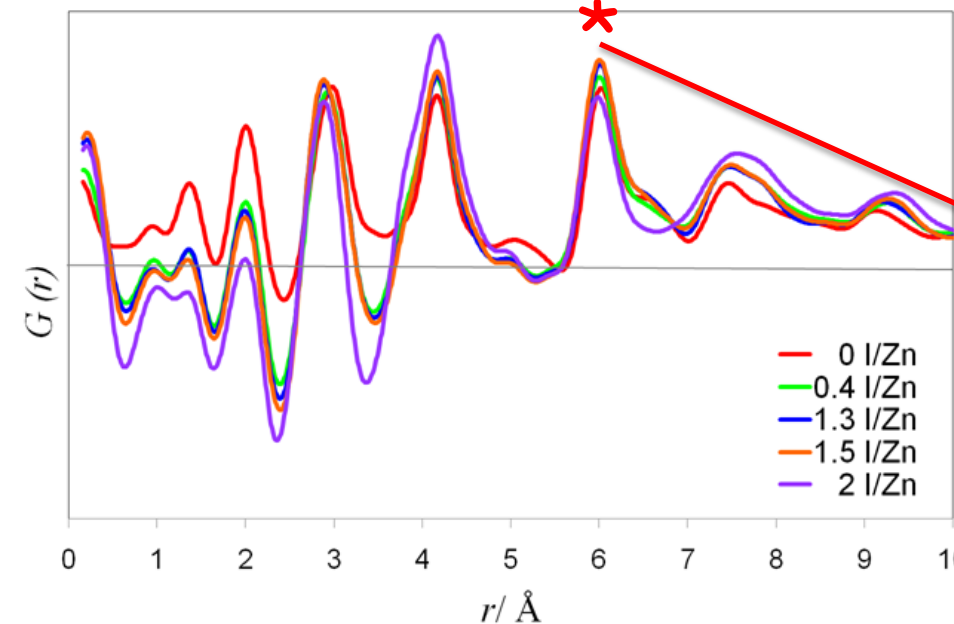
Two distinct I_2 binding sites: I_a and I_b



I_2 site occupancy and $I_2 \cdots$ MeIM close contacts in $I_2 @ ZIF-8$

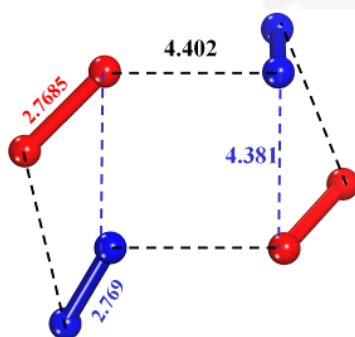
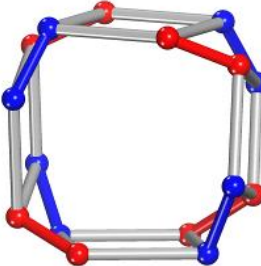
| I_2 site | Site occupancy | Contacts with MeIM |
|------------|------------------------------|------------------------------|
| | 0.4 I/Zn | $C (CH_3)$ |
| I_a | 0.28 | 3.506 Å; 4.823 Å |
| I_b | 0.14 | 3.620 Å; 3.876 Å |
| | | $C(H=CH)$ |
| I_a | 0.88 | 5.268 Å; 6.408 Å |
| I_b | 0.38 | 3.179 Å; 3.526 Å |

Pair Distribution Function analysis: local structure probe

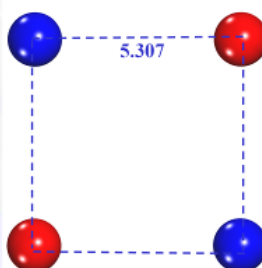
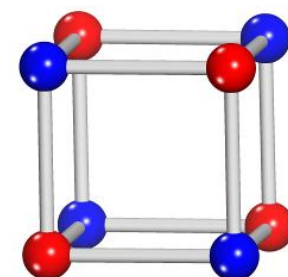
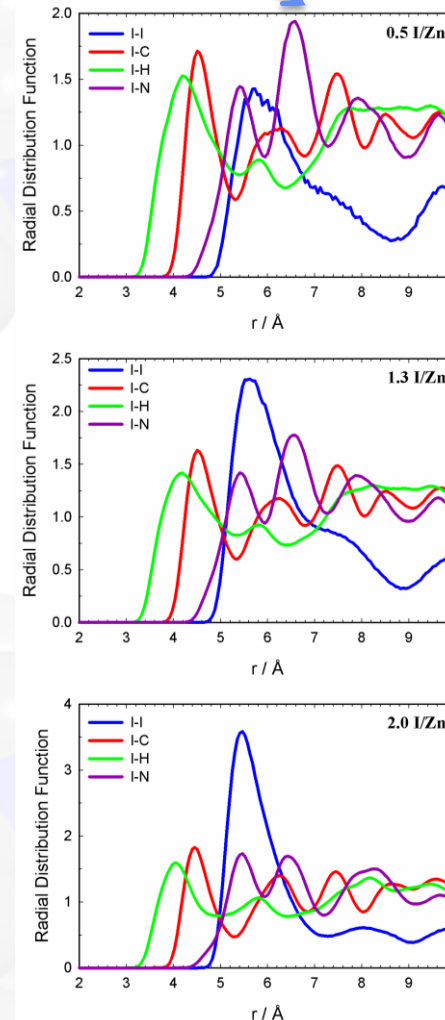
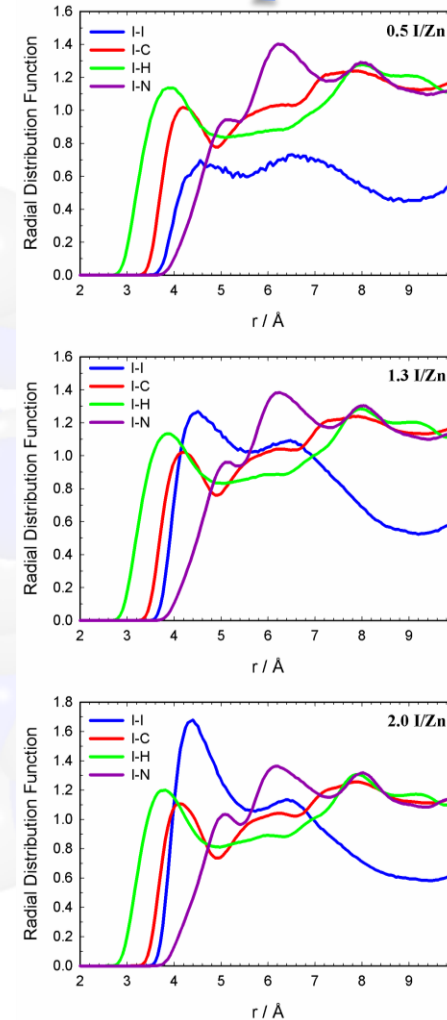


Short-range order and framework connectivity are maintained at all loading levels

- The PDF method- a weighted histogram of the atomic distances, independent of sample crystallinity
- Below $\sim 6 \text{ \AA}$, the MOF cage features are retained in the PDF at all I_2 loading levels
- The persistence of the peak at $\sim 6 \text{ \AA}$, corresponding to the Zn-(MeIM)-Zn' distance
- $>1.3 \text{ I/Zn}$ (70wt%) lose long range structural information though individual cages maintain crystalline integrity

Radial Distribution Functions (RDFs) for
diatomic and united-atom models

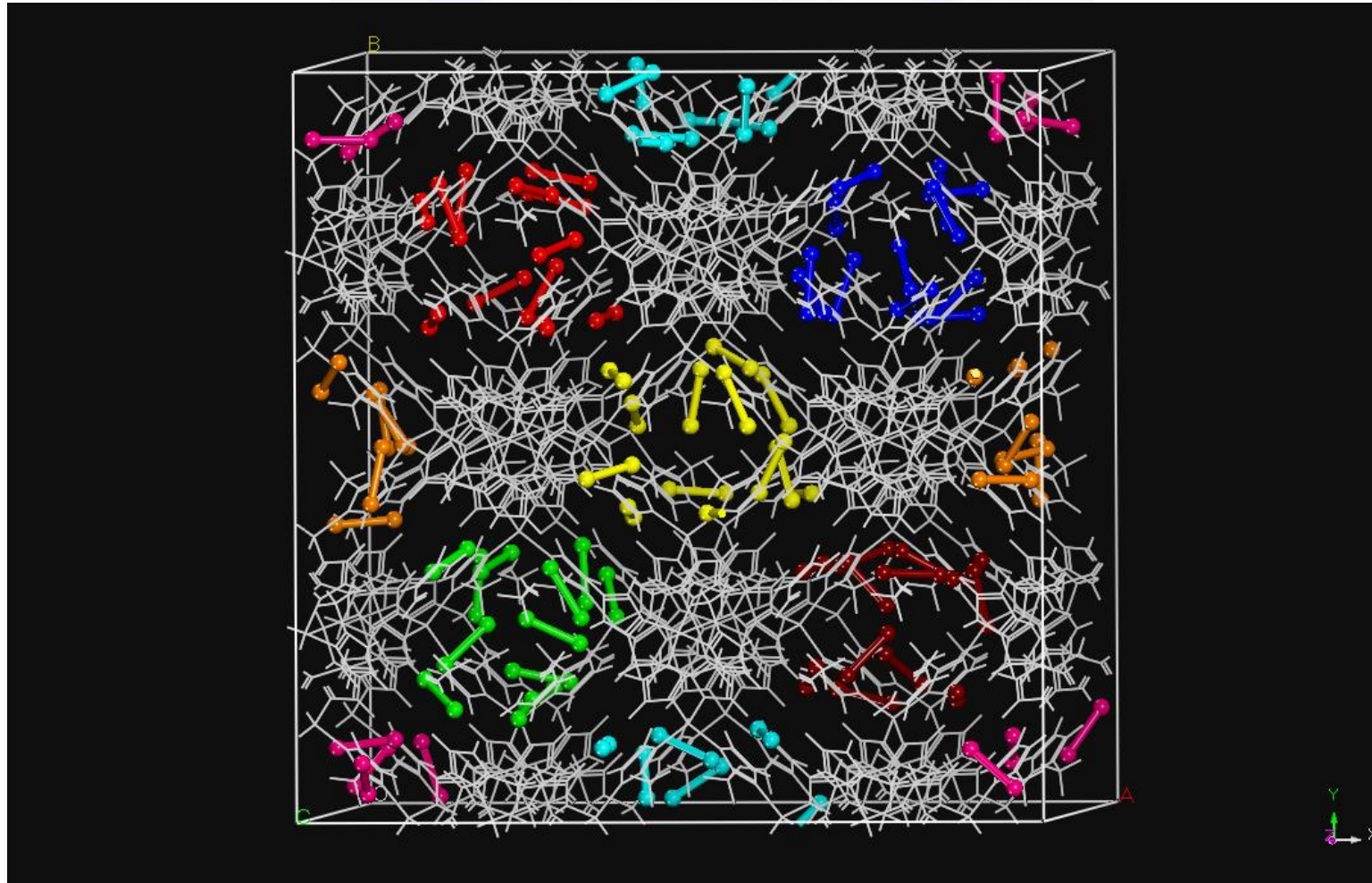
Distorted octagonal prism formed by refined I_2 molecules, and corresponding intermolecular interactions.



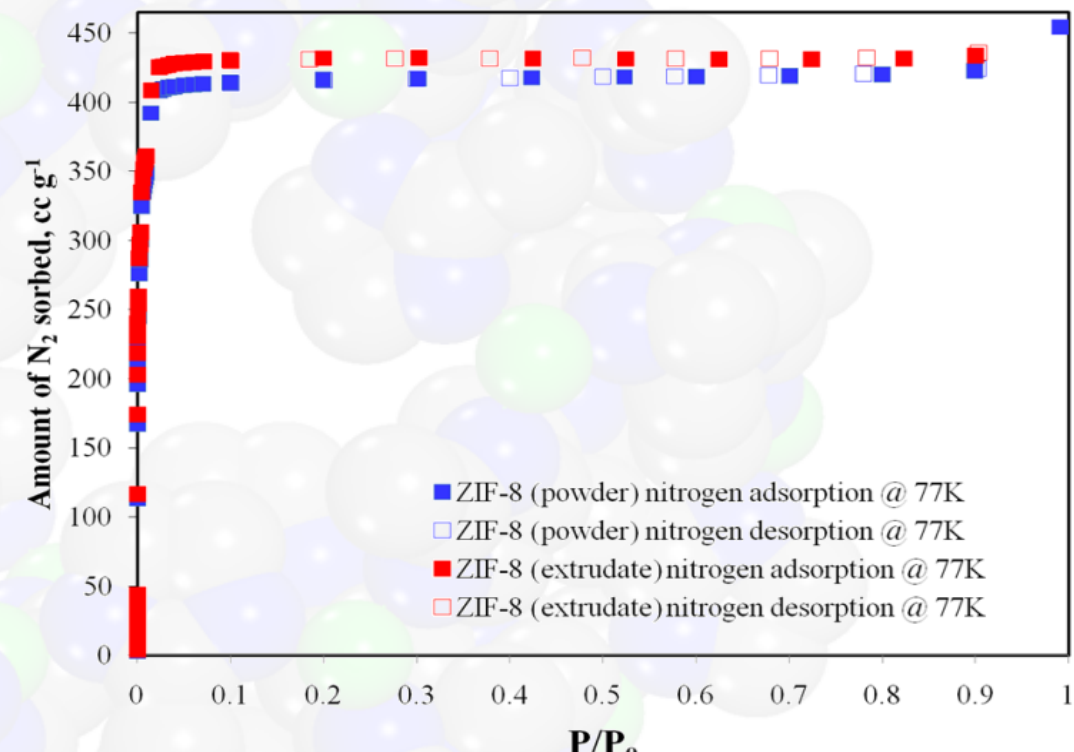
Cubane-like cluster derived from a united-atom model for I_2 , and representative contacts for this molecular arrangement.

Good agreement between crystallography, PDF and modeling regarding nearest neighbors distances

Dynamics of I_2 within cages: I_2 mobility is restricted within individual cages



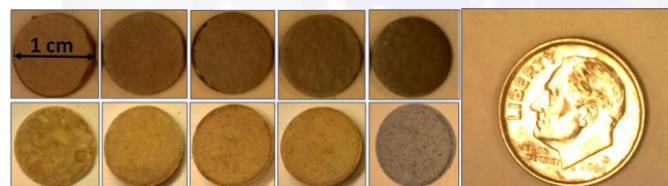
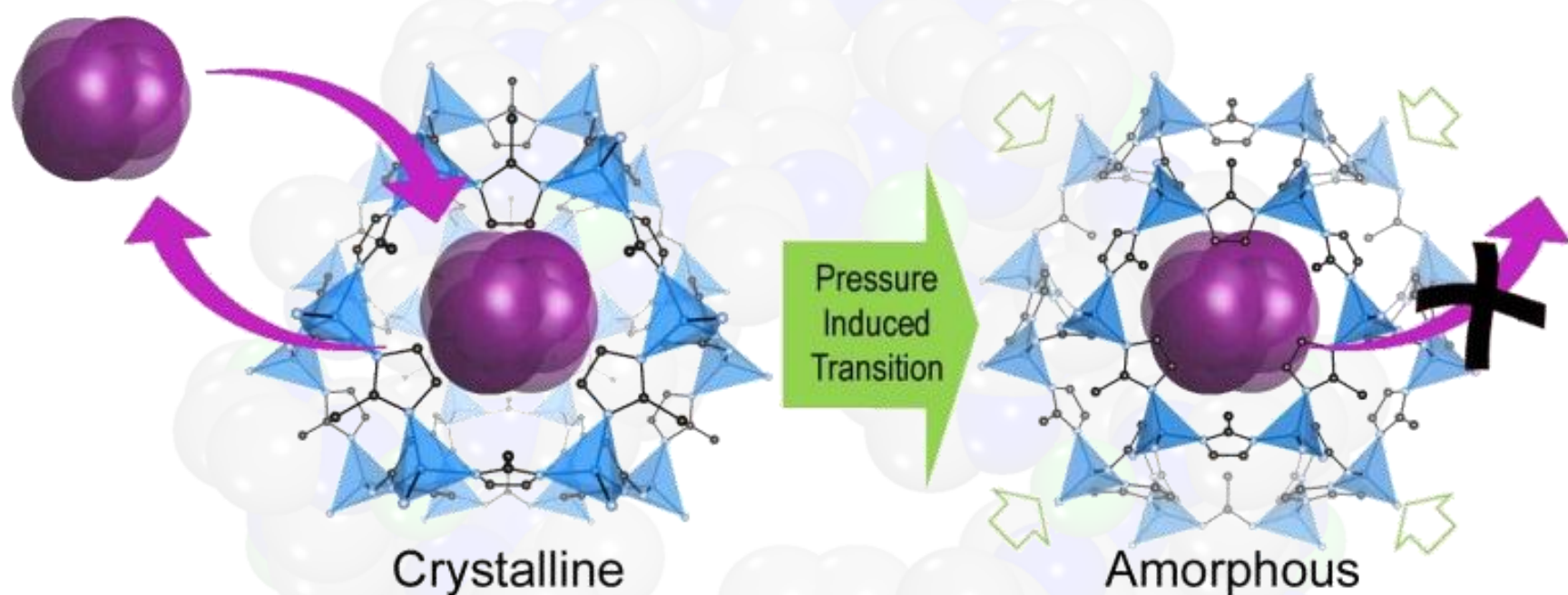
ZIF-8 binder-free extrudates: on par performance with ZIF-8 powder



I₂ loaded extrudates

Technical advance for US Patent # 11971 submitted, 04/2011

IIb. I_2 @ZIF-8 pressure-induced amorphization for capture and temporary storage

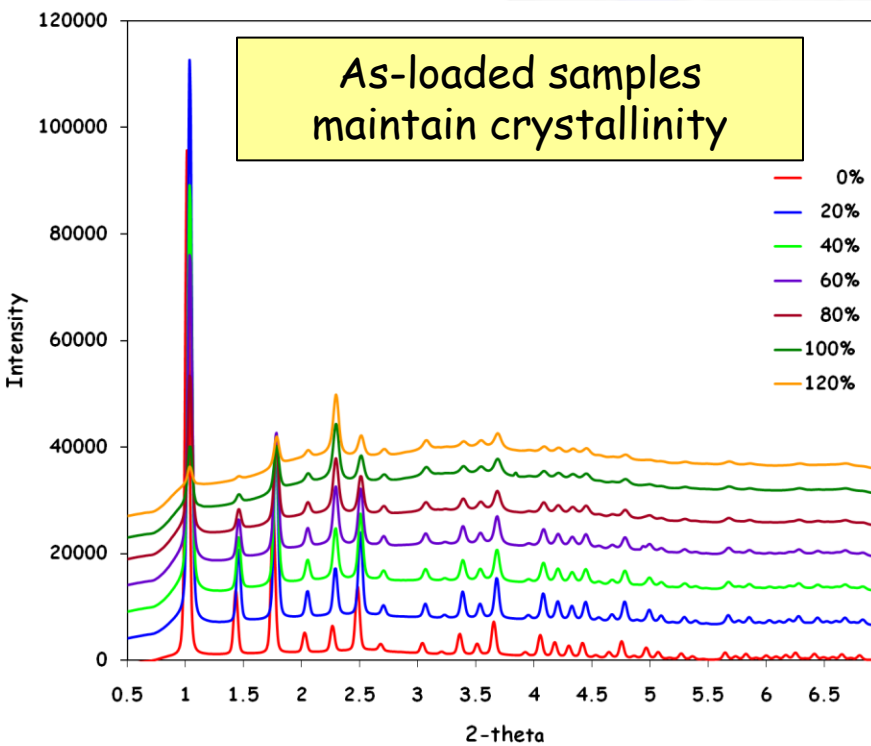


Secure consolidated interim storage
before incorporation into a long term
waste form

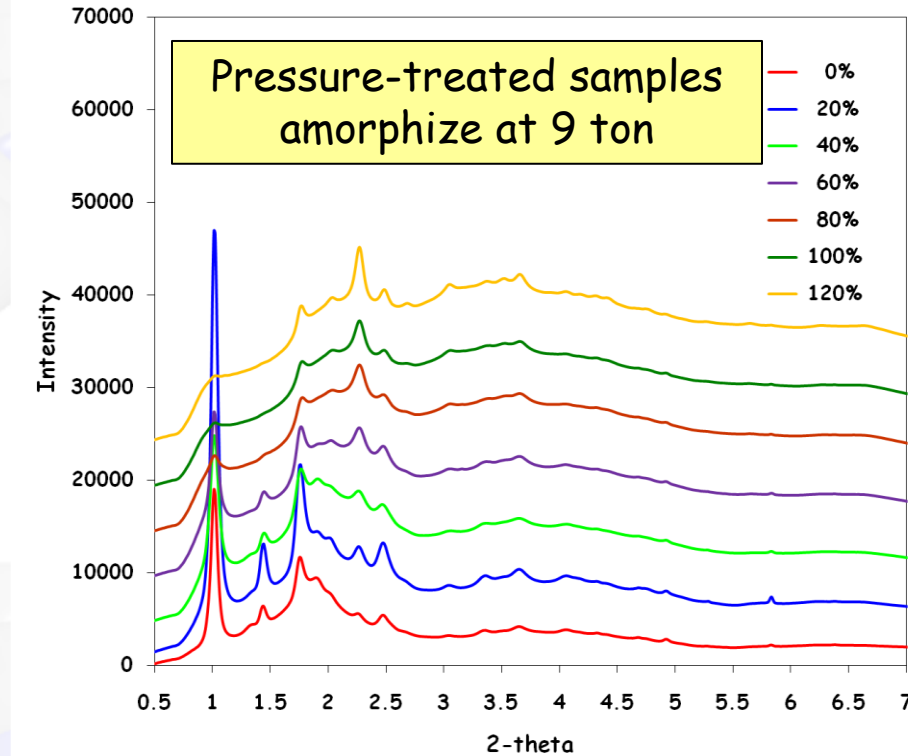
Crack free pellets of iodine loaded ZIF-8 powders
were obtained by applying uniaxial mechanical
pressure.

Chapman, K.W., Sava, D. F. et al *J. Am. Chem. Soc.* 2011, 133 (46), 18583-18585.

High-resolution synchrotron-based XRD on a series of incrementally loaded $\text{I}_2@\text{ZIF-8}$



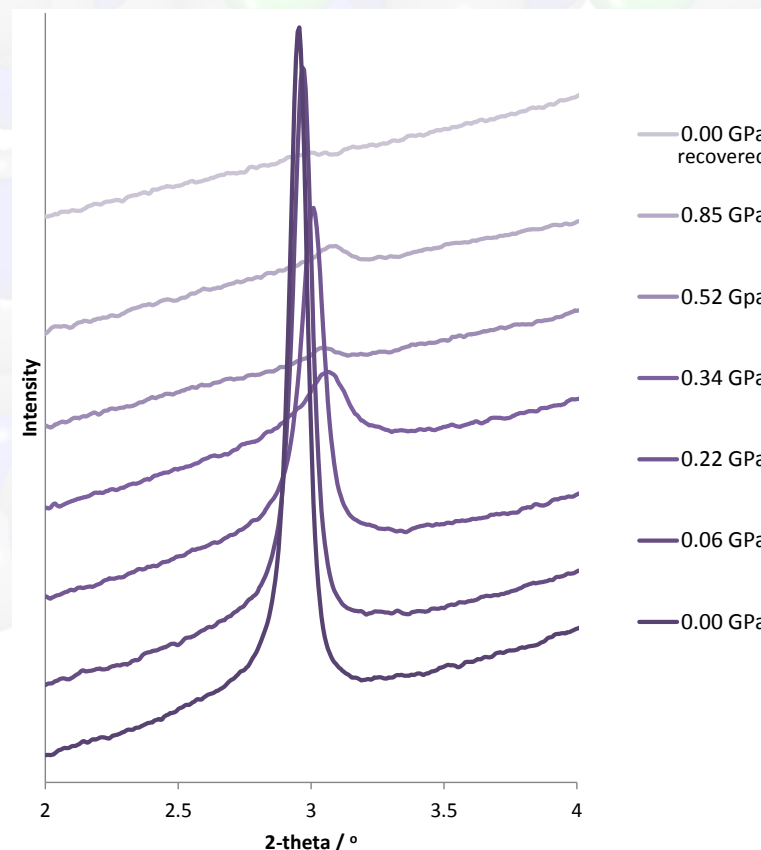
High-resolution synchrotron-based XRD of as-loaded 20, 40, 60, 80, 100 and 120 wt% $\text{I}_2@\text{ZIF-8}$.



High-resolution synchrotron-based XRD of powders treated to 9 ton of 20, 40, 60, 80, 100 and 120 wt% $\text{I}_2@\text{ZIF-8}$.

Variable pressure diffraction studies on $I_2@ZIF-8$

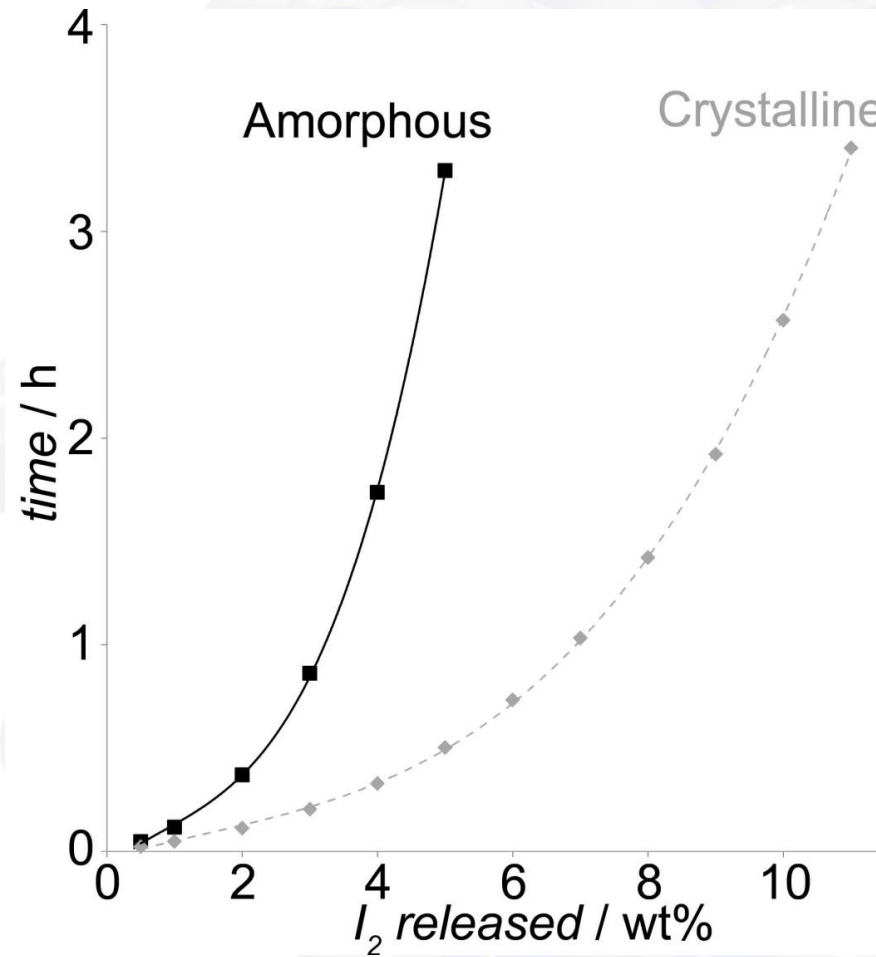
The pressure dependence of I_2 -containing ZIF-8 highlighting the 110 reflection. Above 0.34 GPa, the crystalline diffraction features are largely eliminated and the framework remains amorphous upon recovery to ambient pressure.



- *In-situ* X-ray diffraction were collected at the 1-BM beamline at the APS/ANL.

- The pressure-dependent structure of ZIF-8 loaded with 40wt% I_2 , was probed using synchrotron-based powder diffraction for the sample within a diamond anvil cell pressure apparatus.

Enhanced guest retention through amorphization

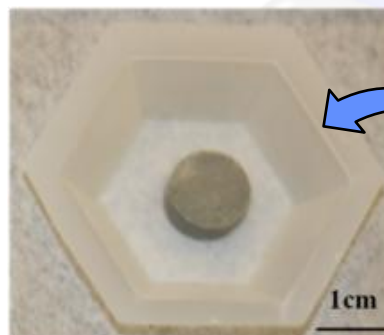


The kinetics of I_2 release from the crystalline and amorphized ZIF-8 based on isothermal TGA data collected at 200°C, 4hours

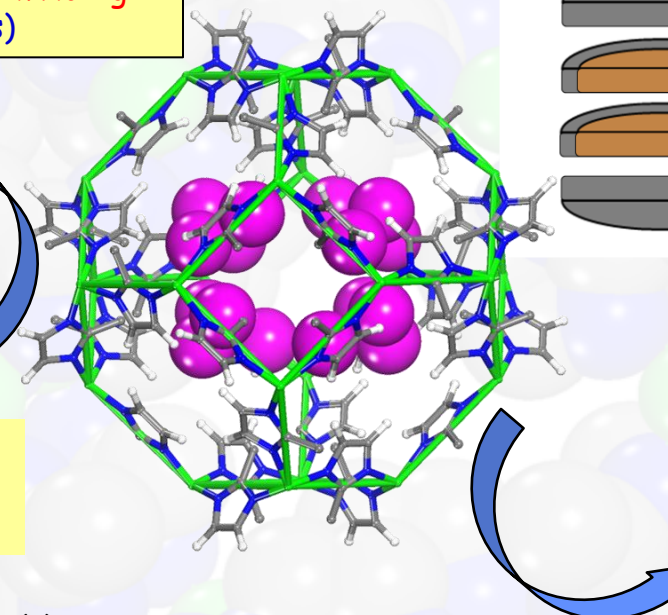
Interim waste form: desorption kinetics are retarded in the amorphized material

IIc. $I_2@ZIF-8$ successfully encapsulated in stable long-term waste forms

Incorporation into Low Temperature Glass Composite Materials (GCM)
80 wt.% glass, 10 wt.% $I_2@MOF$, 10 wt% Ag
(non-optimized compositions)



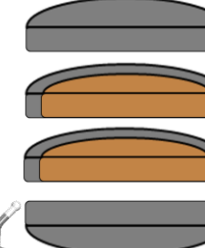
GCM reveal excellent thermal & chemical stability and are appropriate for long term storage



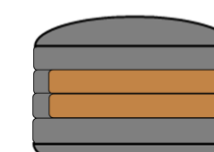
Sava, D.F. et. al *Ind. Eng. Chem. Res.* 2012, 51 (2), 614-620. Invited paper for the thematic Nuclear Energy special issue

TA #SD11720, Provisional Patent 2012

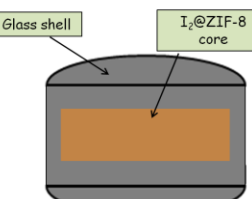
Cross-section of core-shell assembly



Pellets stacking



Core-shell sintering



Very high capacity of consolidated radiological waste

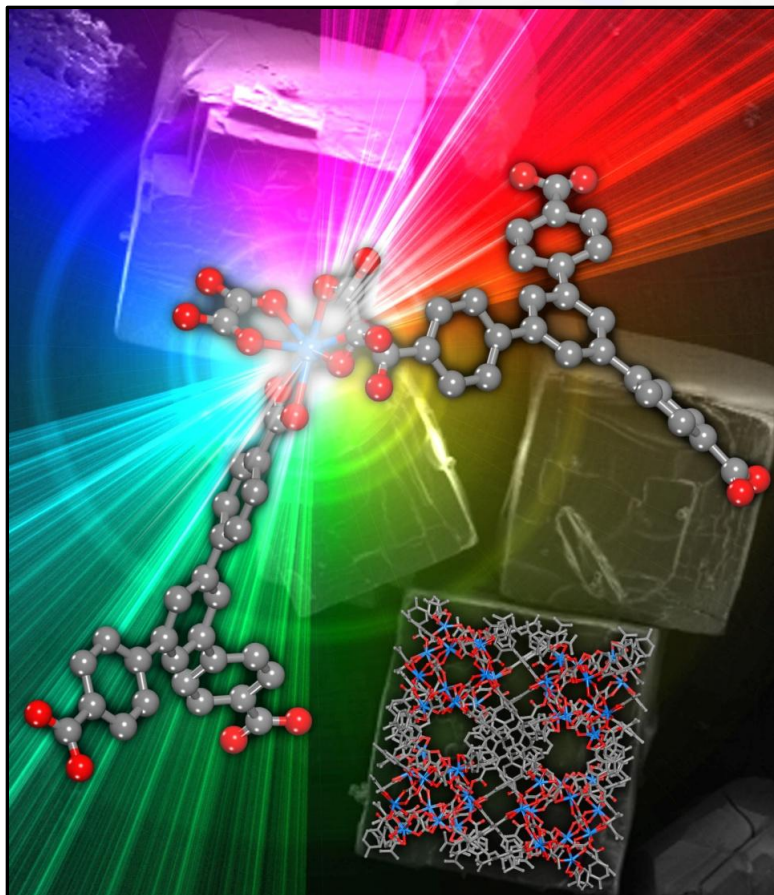


Long-term core-shell waste form

The core consists of amorphized $I_2@ZIF-8$ pellets, and the barrier shell is made of the low-temperature sintering glass EG2922.

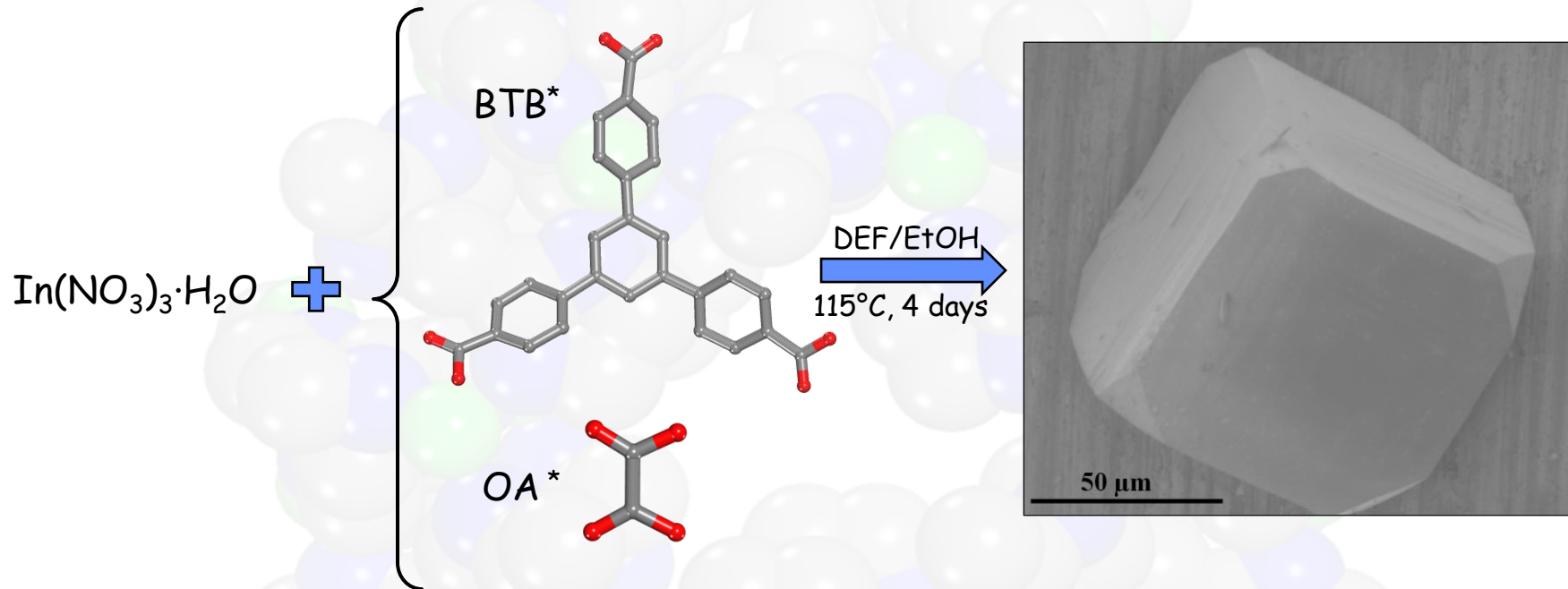
| Glass | ZnO | | Bi_2O_3 | | Al_2O_3 | | SiO_2 | |
|---------|--------|-------|-----------|-------|-----------|-------|---------|-------|
| | mole % | wt. % | mole % | wt. % | mole % | wt. % | mole % | wt. % |
| EG 2922 | 14.2 | 7.8 | 20.2 | 63.4 | 7.8 | 5.4 | 57.8 | 23.4 |

III. Novel MOFs with Tunable Color Properties



- White light from a *single phosphor* - alternatives are sought to existing color mixing approaches
- Current white LEDs for SSL: InGaN LEDs excite a yellow-emitting YAG:Ce phosphor- *cool white light made warmer* by incorporating a red-emitting phosphor
- Warm white LEDs: near-UV InGaN LEDs to excite blends of red-, green-, and blue-emitting phosphors → the additional down-conversion step (near-UV to blue) *significantly lowers the conversion efficiency of the device.*

SMOF-1 (Sandia Metal-Organic Framework-1): a tunable novel In-BTB framework



- ✓ The first In-BTB reported net
- ✓ The first oxalic acid-BTB system explored to date

Cubic, 3-periodic

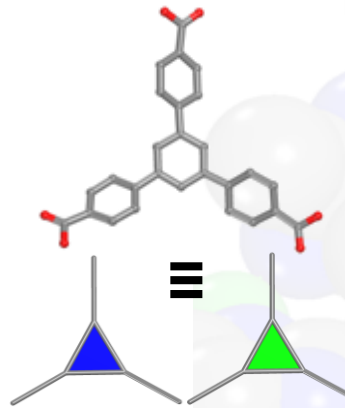
$a = 33.975(3) \text{ \AA}$, Ia-3
 $V = 39,217(10) \text{ \AA}^3$

* BTB (4,4',4'' -benzene-1,3,5-triyl-tri-benzoic acid)
* OA (oxalic acid)

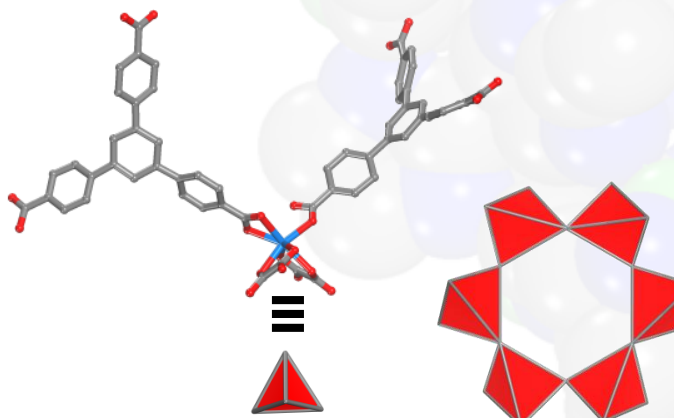
dfsava@sandia.gov

Sava, D.F. et.al, *J. Am. Chem. Soc.* 2012, 134 (9), 3983.

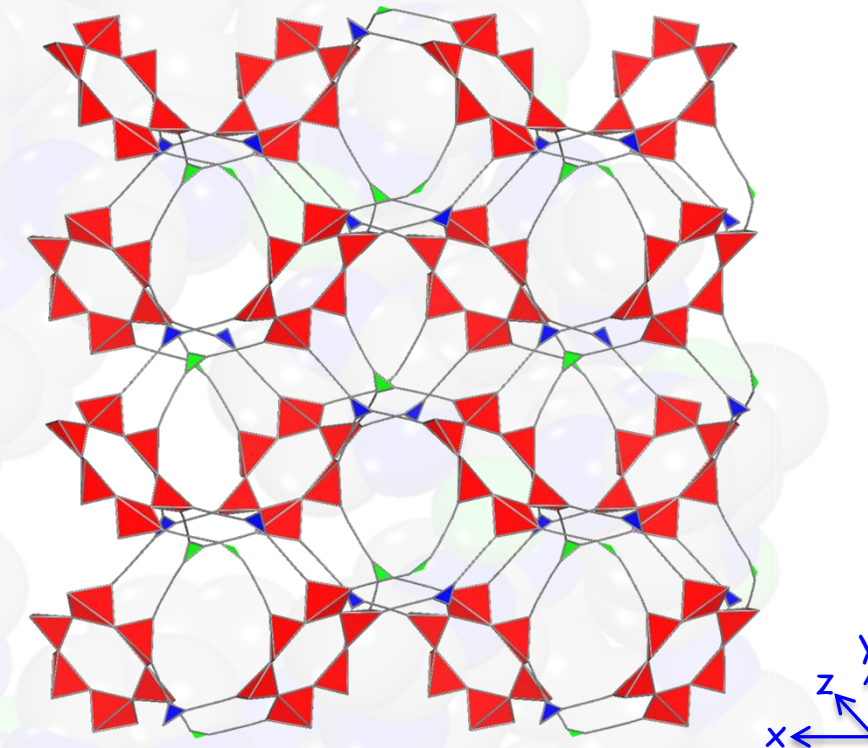
Topological evaluation: unprecedented (3,3,4) trinodal net



Two topologically distinct
3-connected nodes



4-connected node



Coordination sequences:

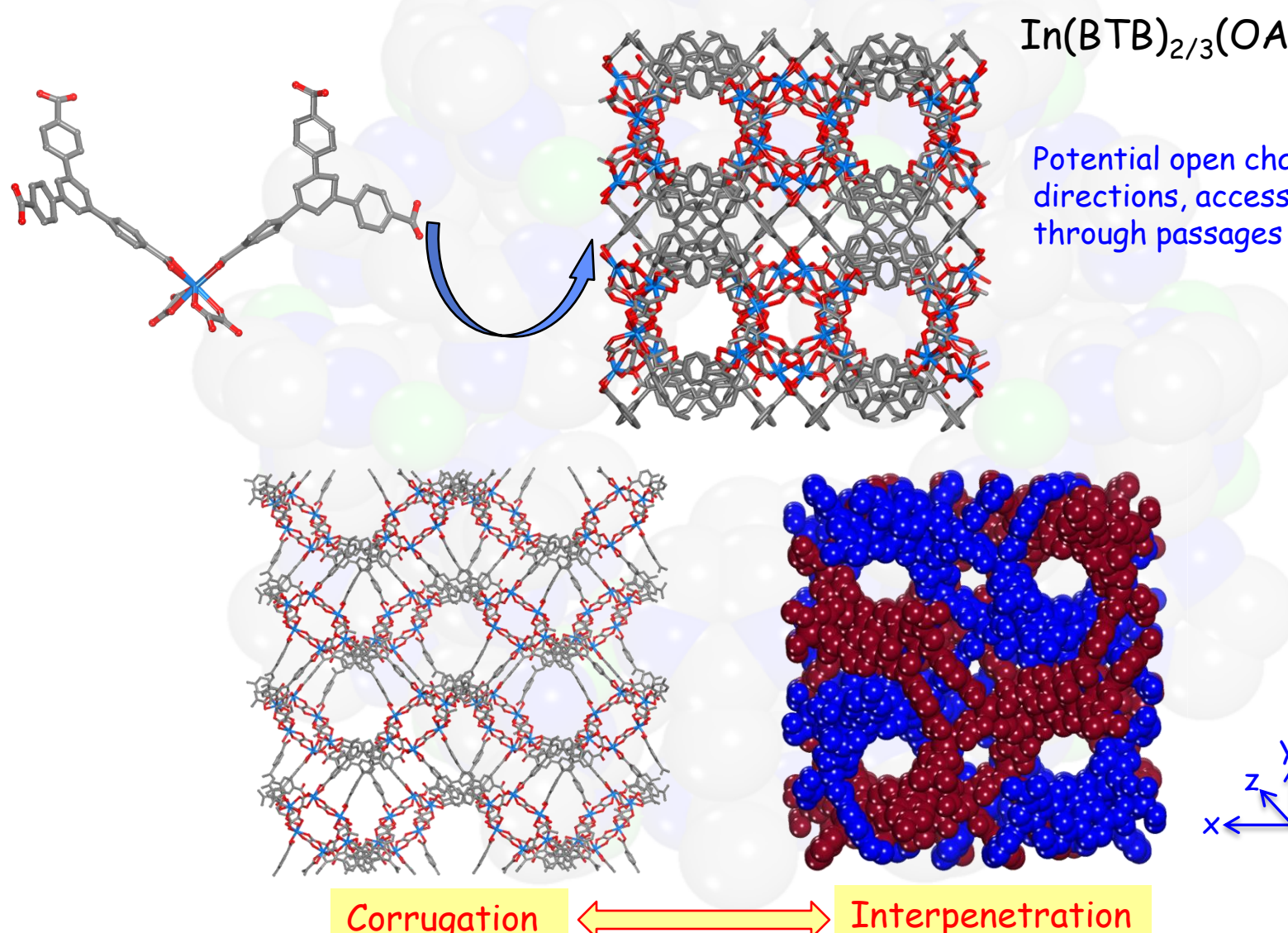
V1: 3 9 22 36 58 88 114 151 196 234

V2: 3 9 22 39 54 79 119 151 186 240

V3: 4 10 21 39 60 85 117 154 195 242

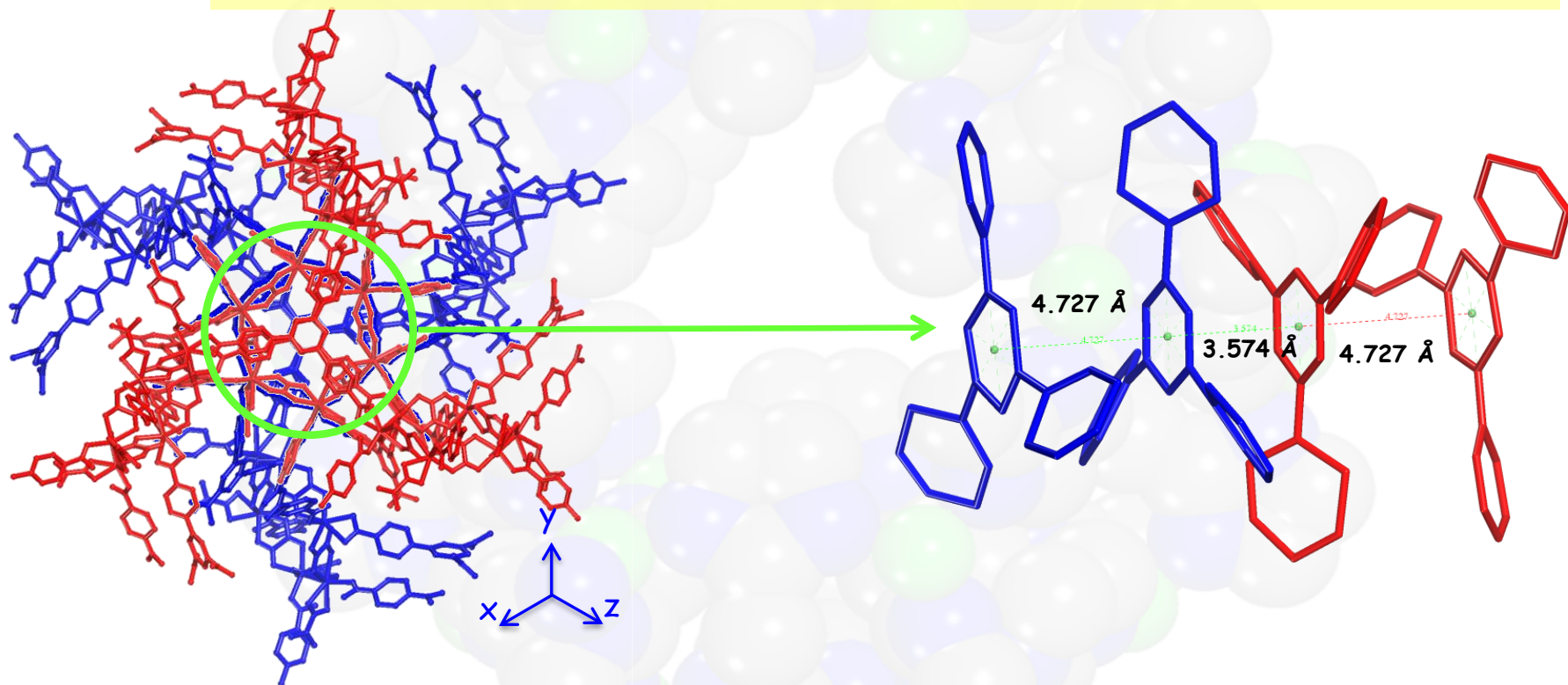
The short Schläfli (point) symbol: $\{6^3.8^3\}3\{6^3\}2$

Complementary structural features direct enhanced linker interactions



Photoluminescence originates from the unique arrangement of the conjugated aromatic rings

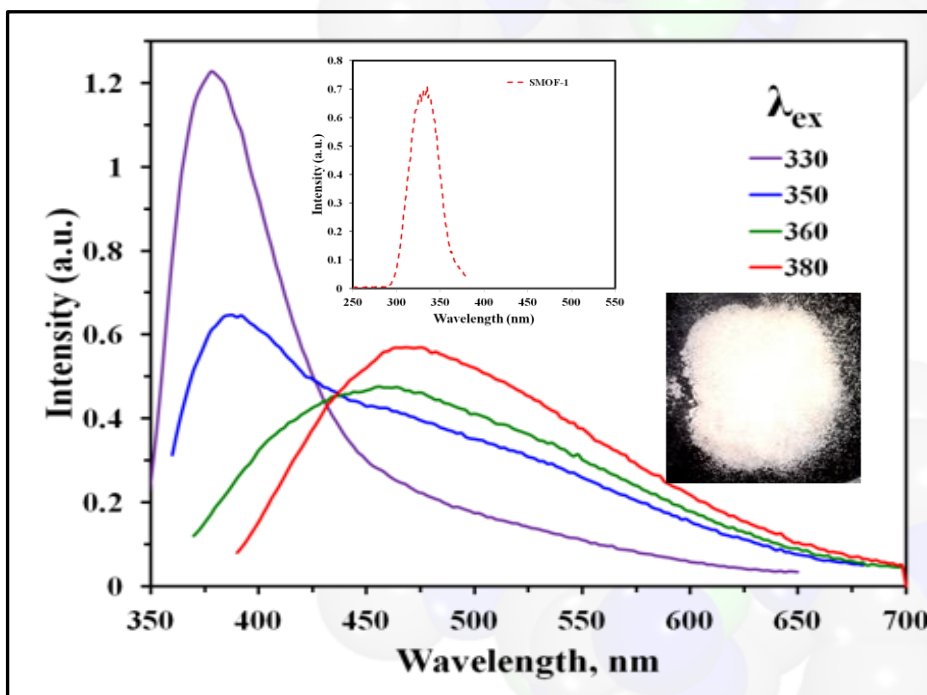
The structure-function relationship in SMOF-1 is driven by two complementary unique structural features: corrugation and interpenetration



Unique arrangement of BTB linkers in SMOF-1 results in a cascade of $\pi-\pi^*$ aromatic interactions

SMOF-1 framework: direct broadband white-light emitter

White-light emission in SMOF-1 is due to a combination of $\pi-\pi^*$ aromatic interactions and ligand to metal charge transfer (LMCT)



Excitation and emission spectra in SMOF-1

Color properties in SMOF-1

| λ_{ex} | CRI* | CCT* (K) | x | y |
|----------------|------|----------|-------|-------|
| 330 | 77.4 | 34463 | 0.209 | 0.193 |
| 350 | 84.5 | 22413 | 0.241 | 0.268 |
| 360 | 85.1 | 33290 | 0.234 | 0.275 |
| 380 | 81.1 | 21642 | 0.235 | 0.387 |

✓ CRI values fall within intended ranges (81-85)

- High CCT (21642-33290 K)

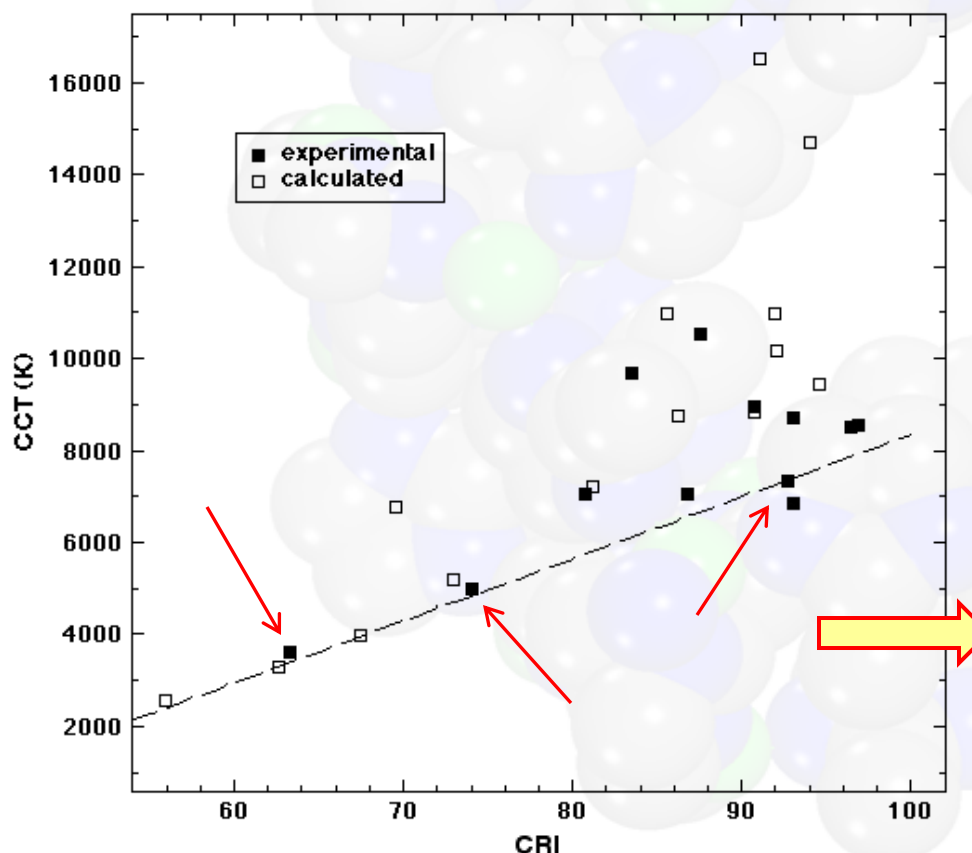
Department of Energy: Solid-State Lighting
<http://www1.eere.energy.gov/buildings/ssl/>

*CRI (Color Rendering Index) ~ 90

*CCT (Correlated Color Temperature) ~ 3200 K

Optimized color properties via simulated spectra

Calculated and experimental CCTs and CRIIs for 2.5, 5, and 10% Eu-doped SMOF-1

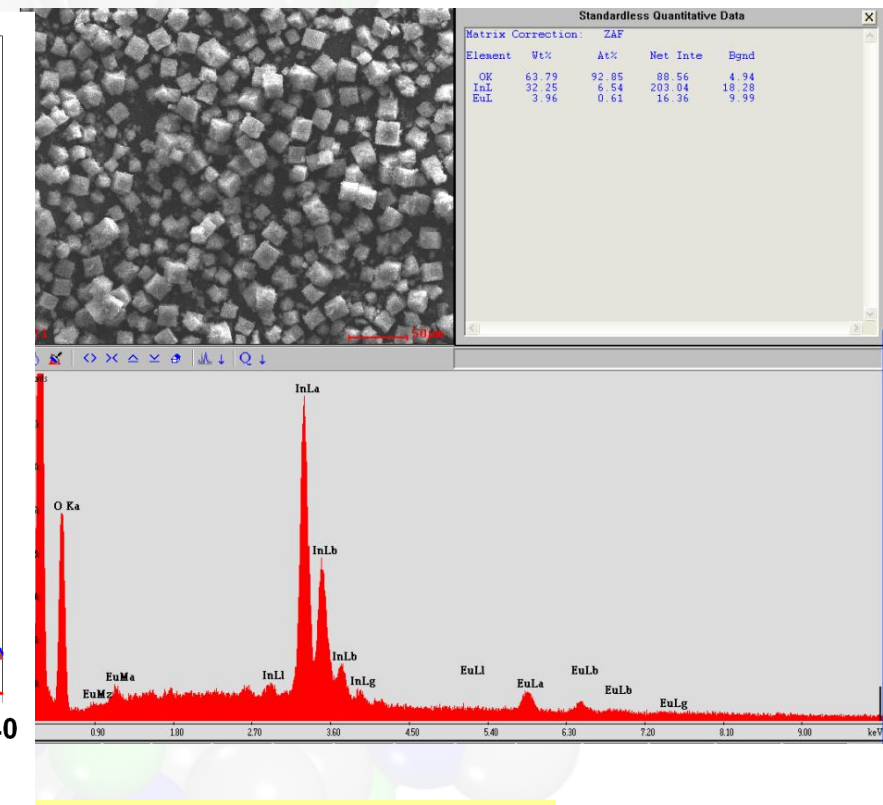
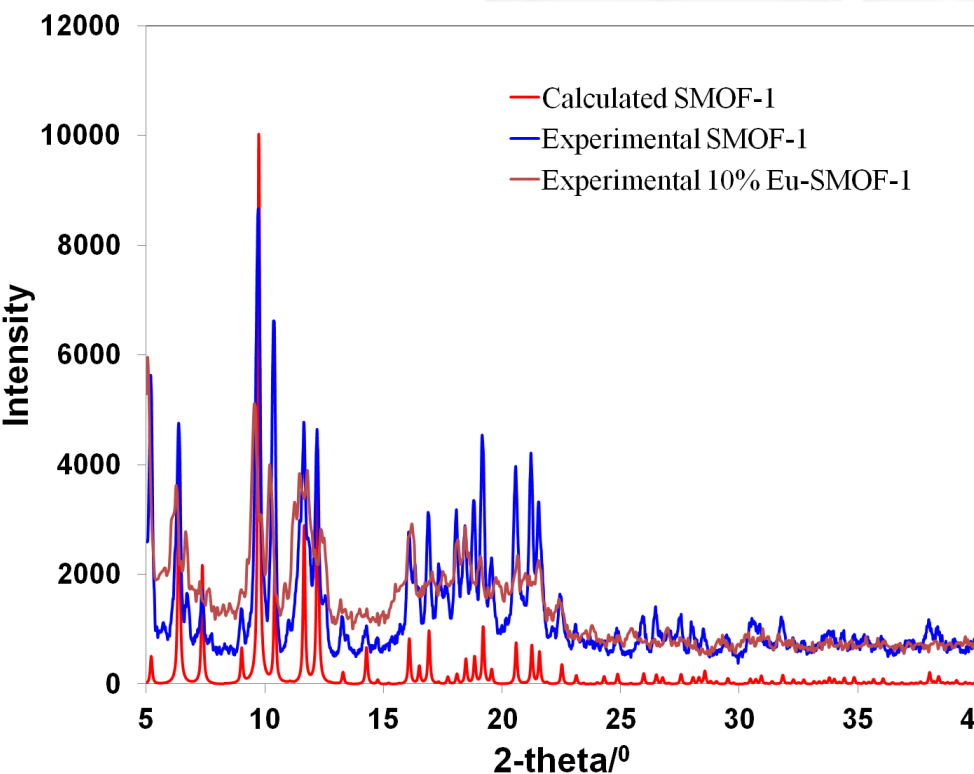


➤ *Simulated spectra* were generated by summing an SMOF-1 and Eu^{3+} spectra, at excitation wavelengths of 350, 360, and 380 nm, respectively.

➤ The best values of CRI and CCT fall *along or below* the dashed line in the plot

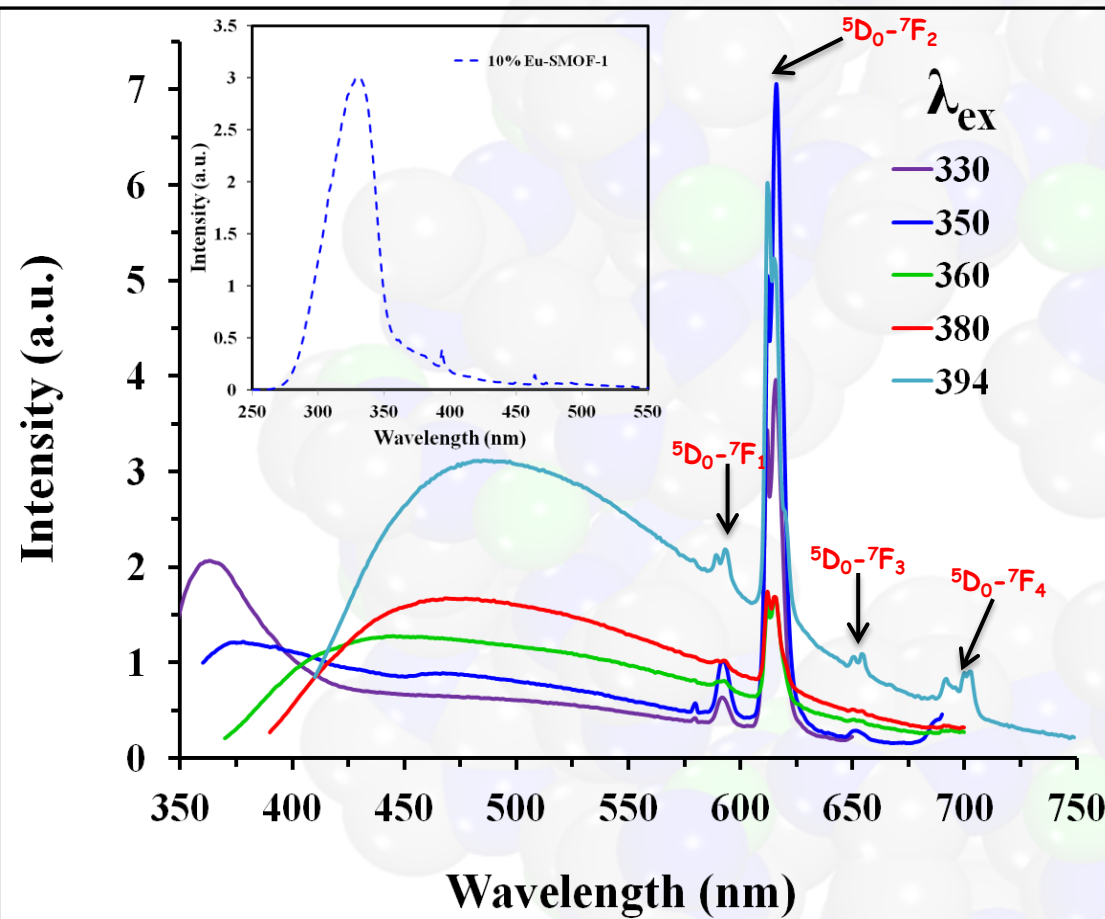
By increasing the Eu^{3+} concentration to 10%, the CRI and CCT shift closer to the set target of $\text{CRI} \sim 90$ and $\text{CCT} \sim 3200\text{K}$

Successful in-framework Eu co-doping at 2.5, 5, and 10%



Unit cell refinement of the 10% Eu-doped SMOF-1 sample reveals *enlarged unit cell parameters* $a=34.57(6)$ Å, compared to $a=33.975(3)$ Å.

Enhanced system tunability: improved color properties with in framework 10% Eu co-doping



Color properties in 10% Eu-doped SMOF-1

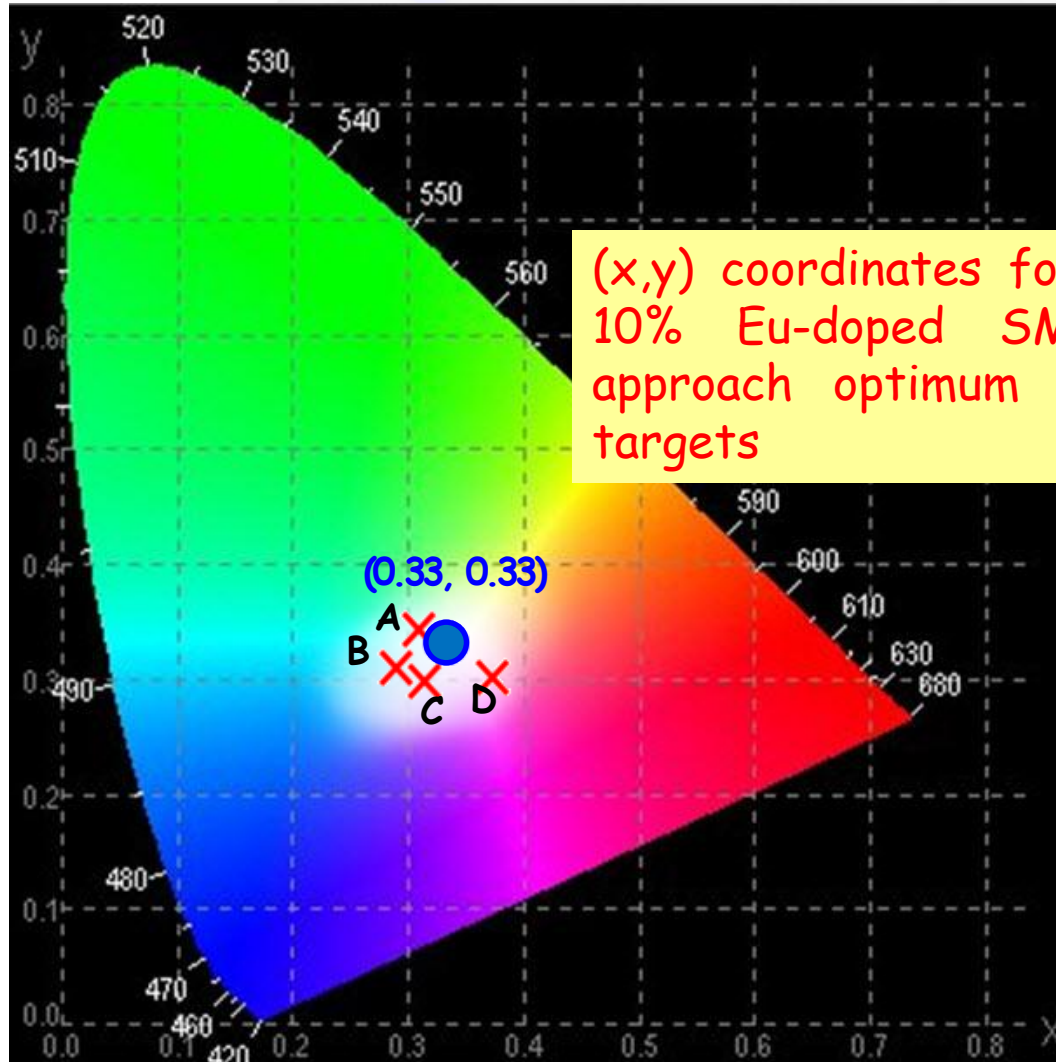
| λ_{ex} | CRI | CCT (K) | x | y |
|----------------|-----|---------|-------|-------|
| 350 | 63 | 3606 | 0.369 | 0.301 |
| 360 | 81 | 7068 | 0.309 | 0.298 |
| 380 | 93 | 8695 | 0.285 | 0.309 |
| 394 | 93 | 6839 | 0.304 | 0.343 |

✓ CCT values are significantly improved

Narrowband emission peaks observed from the Eu^{3+} component, attributed to the parity forbidden $^5D-^7F$ transitions

Absolute QY $\sim 4.3\%$ at 330nm

CIE* optimum white-light chromaticity coordinates: (0.33, 0.33)

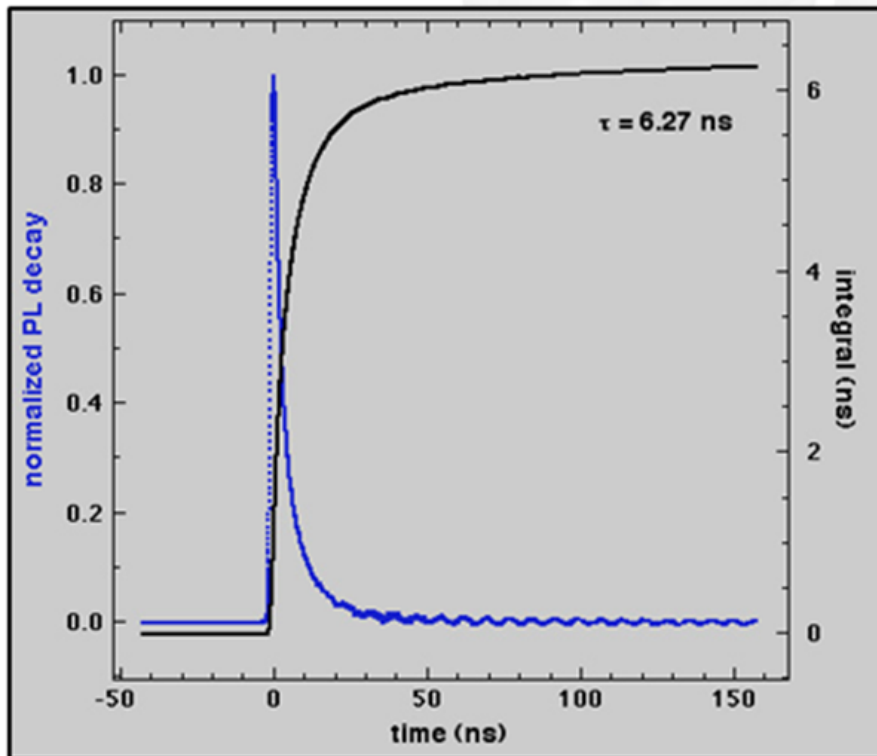


*CIE: Commission
Internationale de l'Eclairage

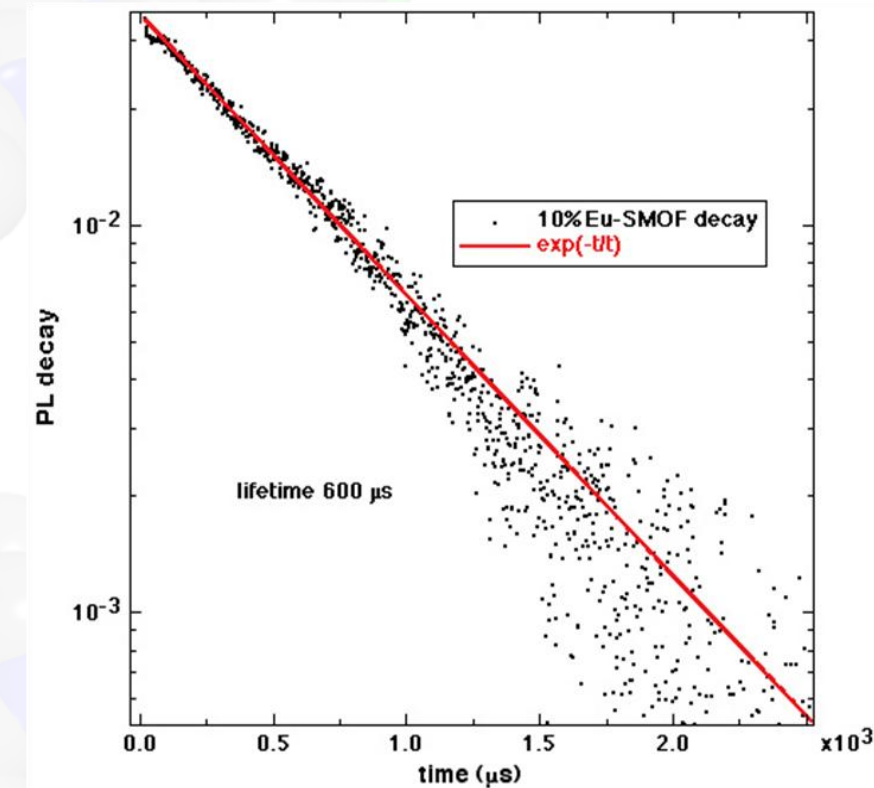
(x,y) coordinates for the
10% Eu-doped SMOF-1
approach optimum CIE
targets

A-D: (x, y) chromaticity coordinates
for $\lambda_{ex} = 394, 380, 360, 350$ nm.

Framework tunability is reflected in the PL lifetime



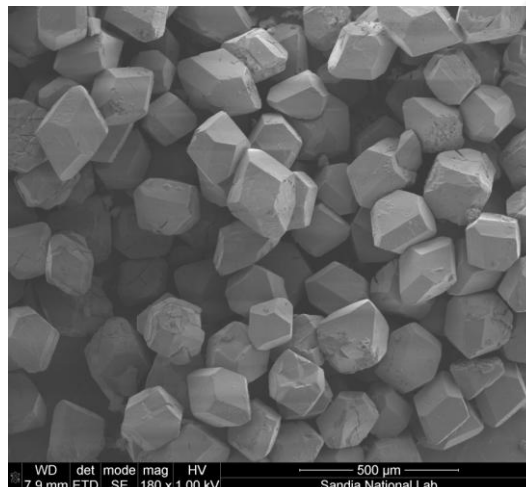
SMOF-1 harmonic
average lifetime **6.27 ns**



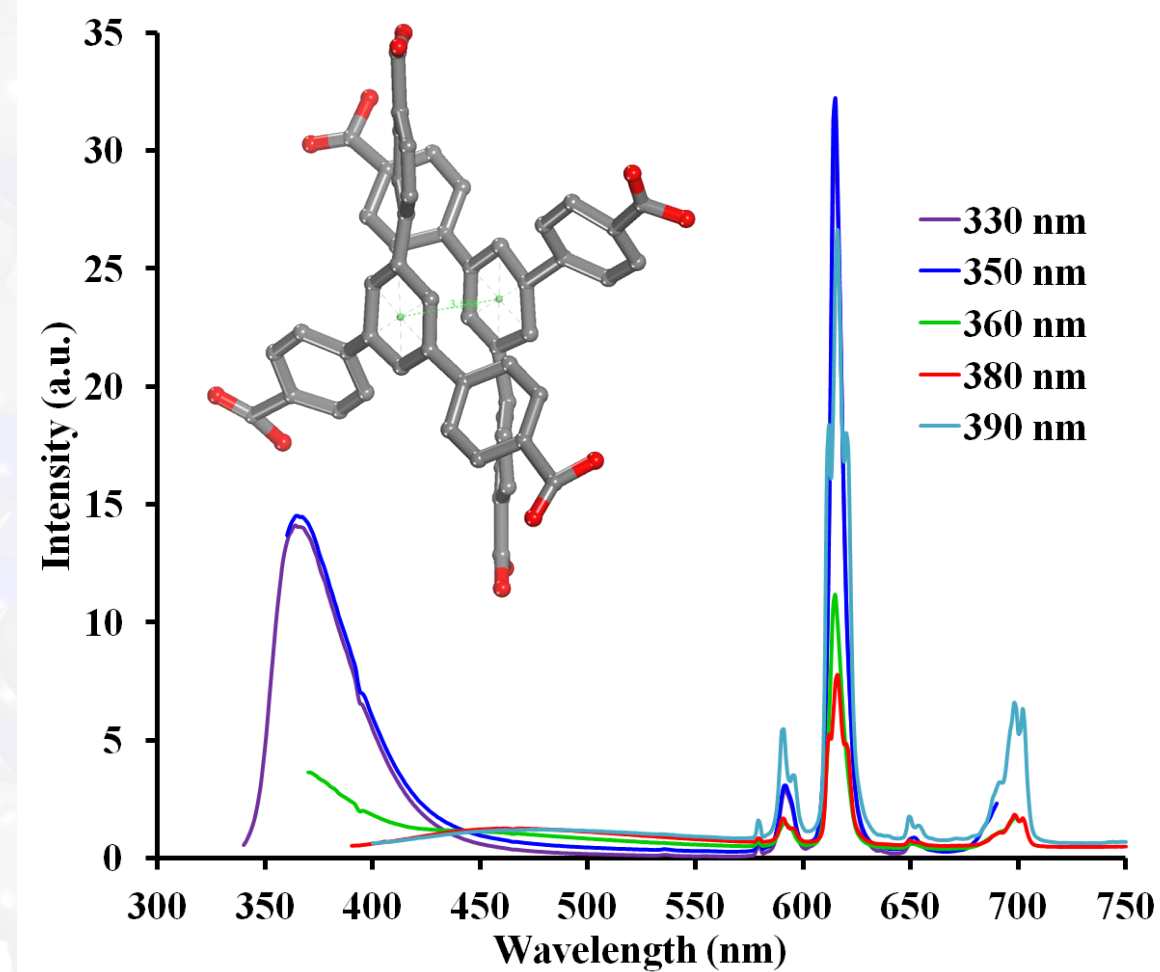
10% doped Eu-SMOF-1 harmonic
average lifetime **600 μs**

On-going studies

SMOF-2: a novel In-30% Eu- BTB framework red emitter



$a = b = 43.671 \text{ \AA}$
 $c = 41.867 \text{ \AA}$
 $\alpha = \beta = 90^\circ$
 $\gamma = 120^\circ$
Volume = 69149.5 \AA^3

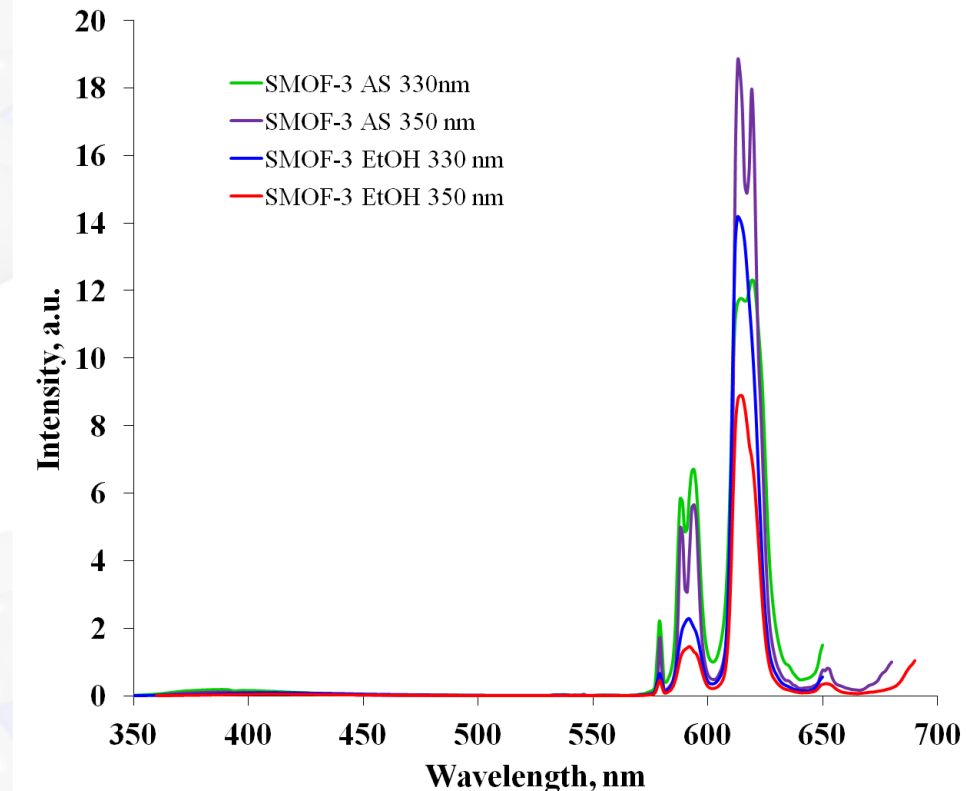
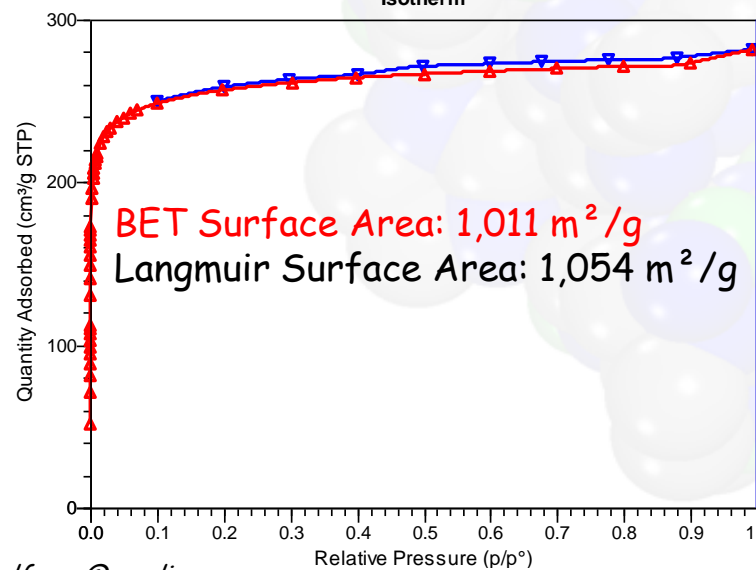
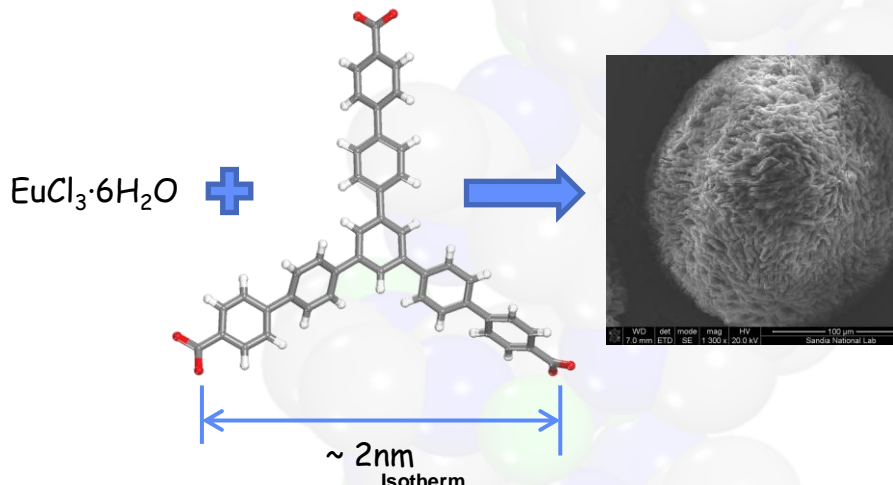


Absolute QY increases to $\sim 11.2 \%$

SMOF-3: a novel Eu-TCBB framework red emitter

SMOF-3:

> 115 wt% I₂ sorption ability (non-optimized)



Absolute QY ~ 21 %

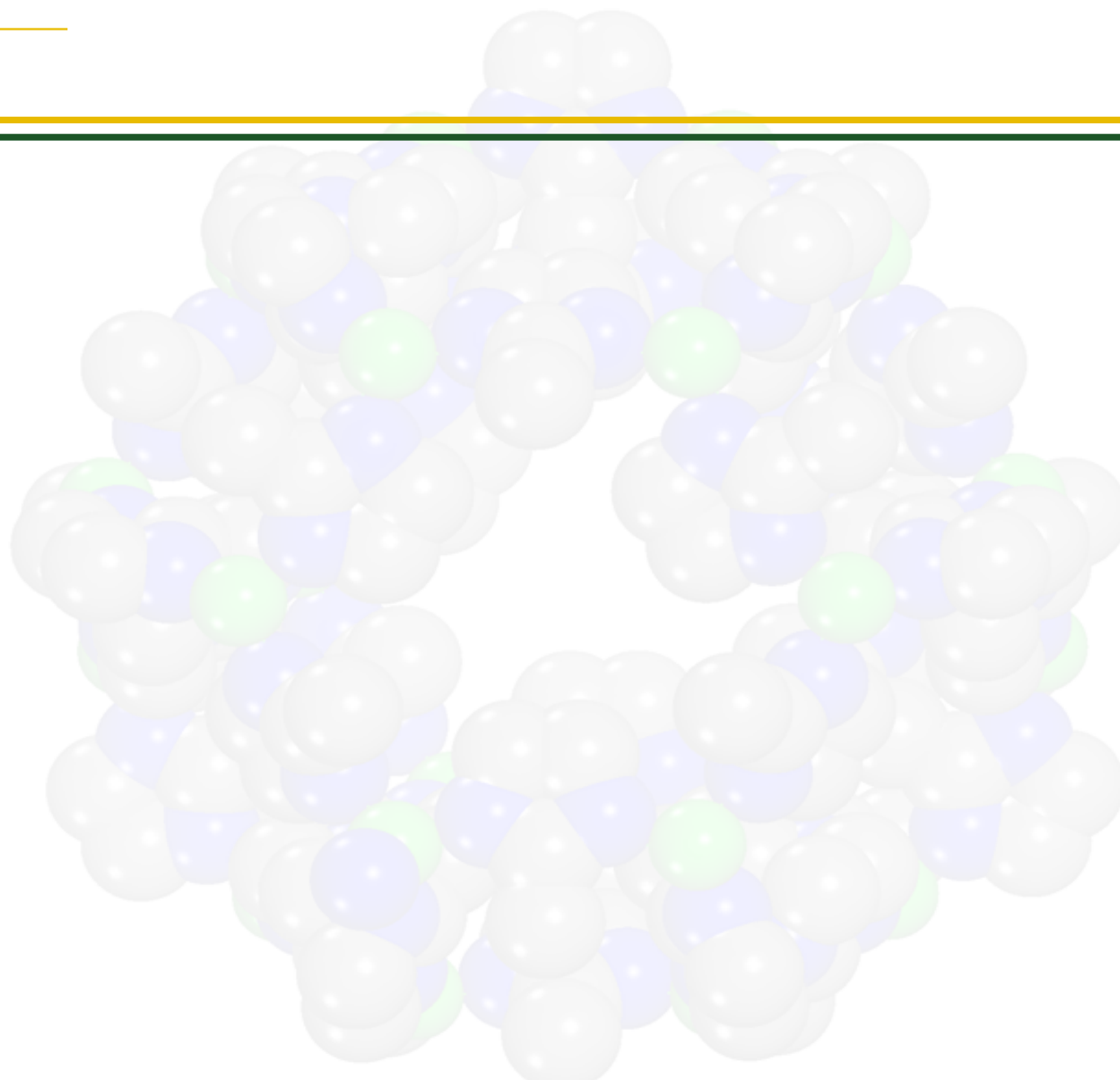
Summary and On-going studies

- MOFs modularity and tunability allows for a variety of energy related applications
- Introduced MOFs in nuclear waste remediation and demonstrated that ZIF-8 is an appropriate candidate for I_2 capture and interim storage
- I_2 is retained in ZIF-8 under amorphizing conditions providing for *consolidated secure interim storage* before incorporation into a long term waste form, ensuring non-contamination of the environment
- Developed a prototype novel MOF material featuring intrinsic broadband direct white light emission and derived a tunable platform which allows for the modifications of associated color properties
- Incorporation of MD simulations and GCMC modeling with structure analysis to study
 - competitive gas sorption from industrially relevant complex streams
 - establish binding locations, mechanisms of sorption and transport in HKUST-1 vs. ZIF-8
- On-going studies into novel MOFs, as well as pre- or post-synthesis framework functionalization for enhanced absolute quantum yields

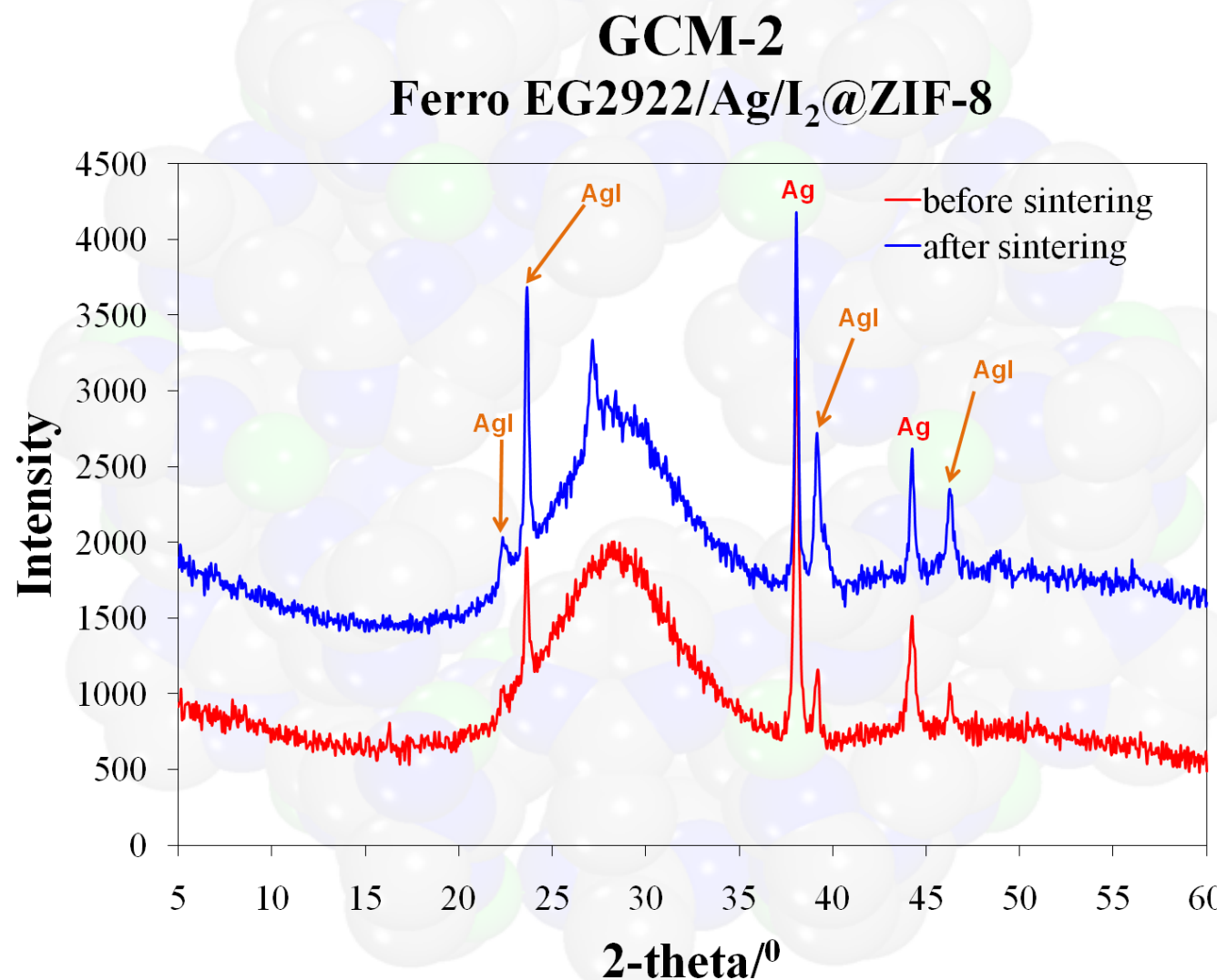


U.S. DEPARTMENT OF
ENERGY

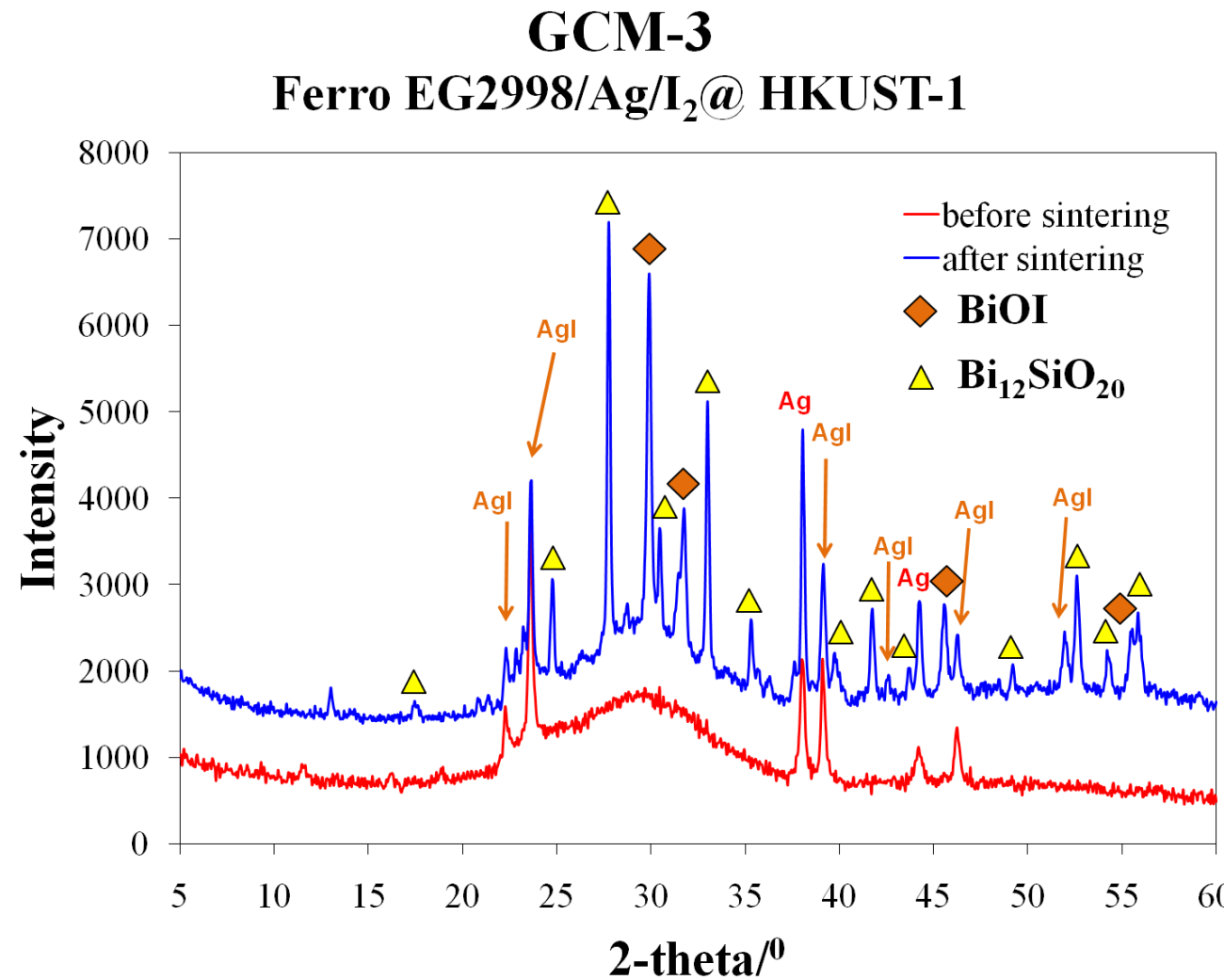
Nuclear Energy



Powder X-ray diffraction pattern for GCM-2 before and after thermal treatment



Powder X-ray diffraction pattern for GCM-3 before and after thermal treatment



Bi-Zn oxide low-temperature sintering glasses

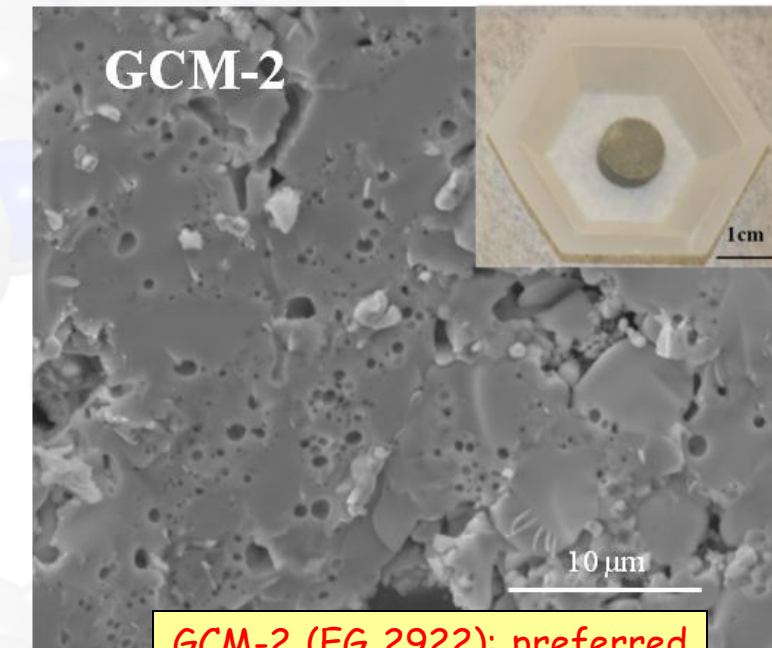
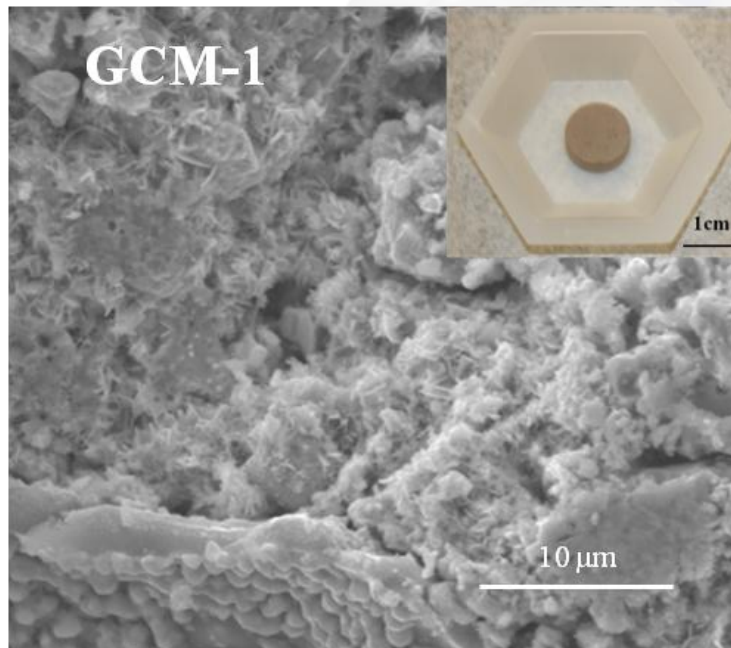


80 wt.% glass, 10 wt.%
I₂@MOF, 10 wt% Ag
(non-optimized compositions)

| Glass characteristics | *EG2998 | *EG2922 |
|-----------------------|-------------------------|------------------------|
| Composition | Bi-Zn-B | Bi-Zn-Si |
| Sintering temperature | 500°C | 525°C-550°C |
| Crystallinity | Crystallizing | Vitreous |
| Density | 5.65 g cc ⁻¹ | 5.8 g cc ⁻¹ |

| Glass | ZnO | | Bi ₂ O ₃ | | Al ₂ O ₃ | | B ₂ O ₃ | | SiO ₂ | |
|---------|--------|-------|--------------------------------|-------|--------------------------------|-------|-------------------------------|-------|------------------|-------|
| | mole % | wt. % | mole % | wt. % | mole % | wt. % | mole % | wt. % | mole % | wt. % |
| EG 2922 | 14.2 | 7.8 | 20.2 | 63.4 | 7.8 | 5.4 | | | 57.8 | 23.4 |
| EG 2998 | 49.7 | 26.9 | 18.9 | 58.6 | | | 31.3 | 14.5 | | |

I_2 @ZIF-8 successfully encapsulated in stable long-term waste forms

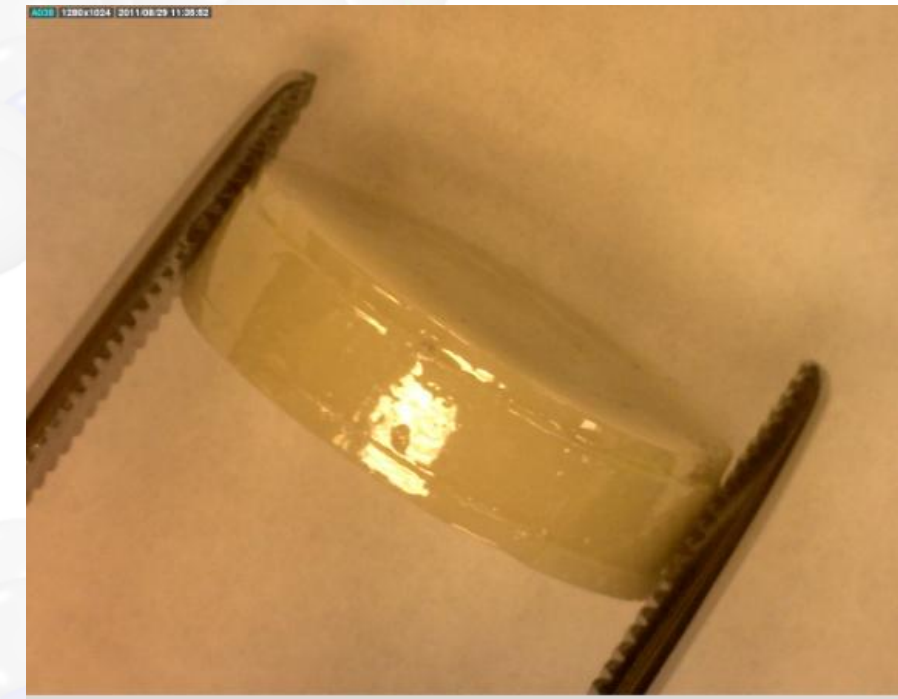
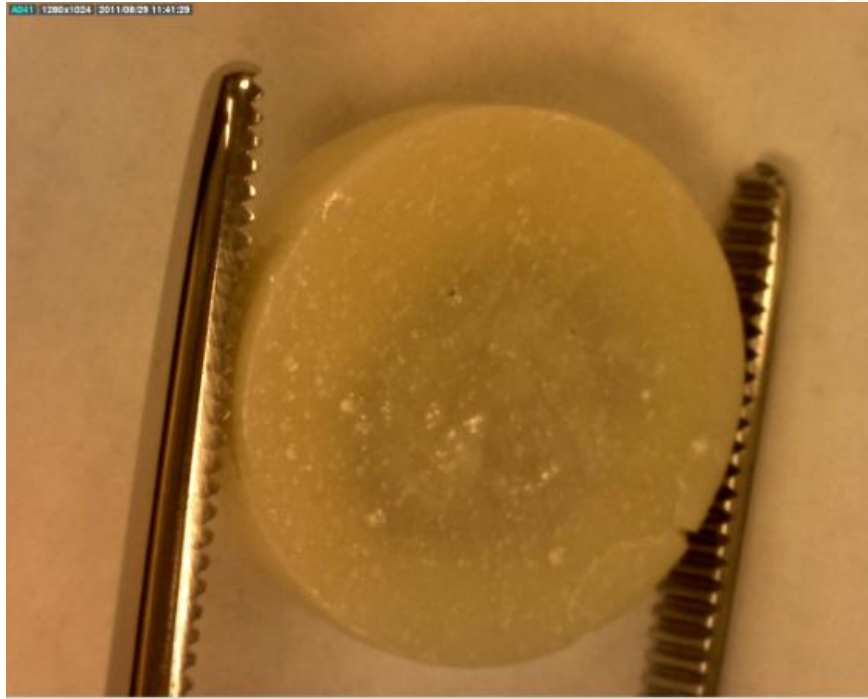


GCM-2 (EG 2922): preferred waste form based on higher leach durability studies

GCM reveal excellent thermal & chemical stability and are appropriate for long term storage: little to no I_2 is lost during processing or after undergoing leach durability studies

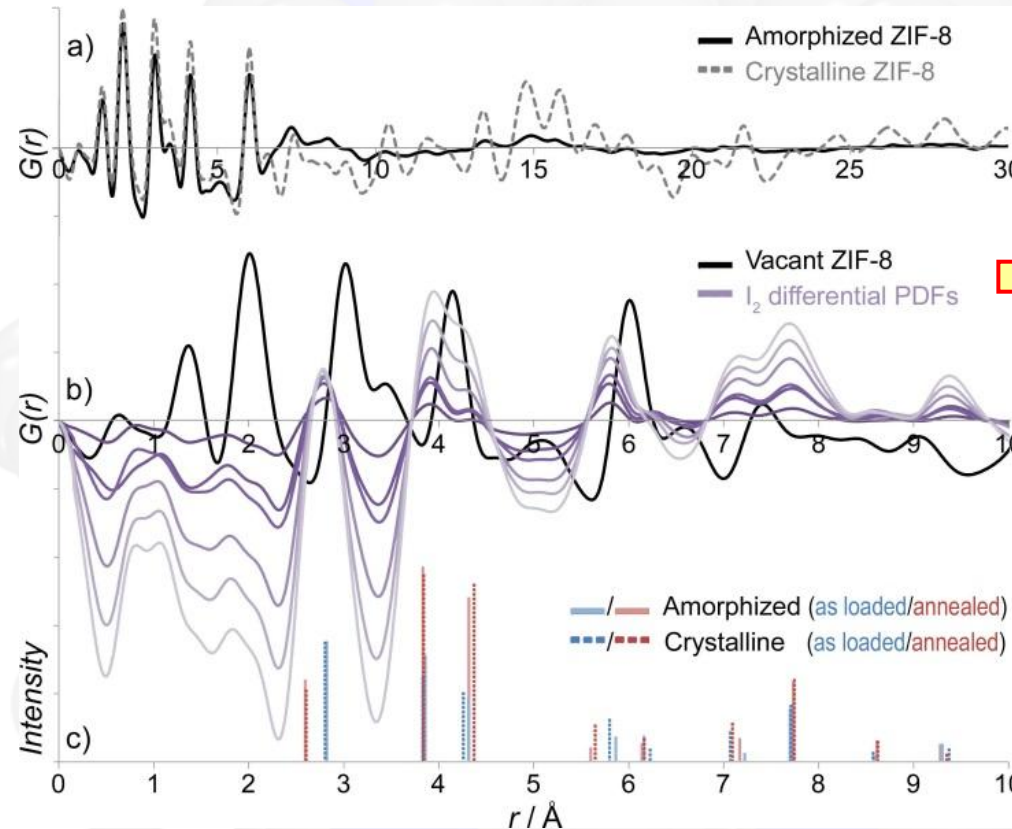
Sava, D.F. et. al *Ind. Eng. Chem. Res.* 2012, 51 (2), 614-620.
invited paper for the thematic Nuclear Energy special issue

Successful sintering of core-shell structures containing amorphized I_2 @ZIF-8 pellets



Compact monoliths comprise high-capacity consolidated radiological waste content for extended storage (1 pellet); scale up to date: 5 pellets per shell

The short-range I \cdots I and I \cdots framework interactions remain unchanged upon amorphization



The framework retains I₂ after pressure treatment

High resolution synchrotron PDFs and differential PDFs collected at APS/ANL for the crystalline and amorphous materials